

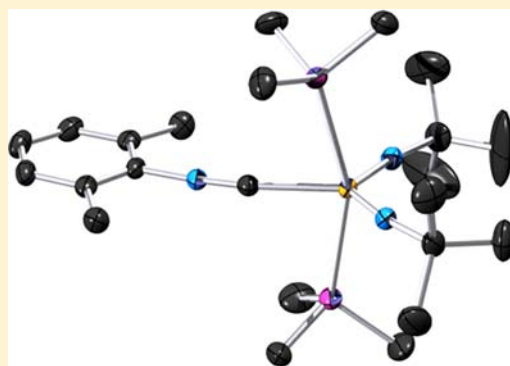
# Carbon Monoxide, Isocyanide, and Nitrile Complexes of Cationic, $d^0$ Vanadium Bisimides: $\pi$ -Back Bonding Derived from the $\pi$ Symmetry, Bonding Metal Bisimido Ligand Orbitals

Henry S. La Pierre, John Arnold,\* Robert G. Bergman,\* and F. Dean Toste\*

Department of Chemistry, University of California, Berkeley, California 94720-1460, United States

## S Supporting Information

**ABSTRACT:** A series of carbon monoxide, isocyanide, and nitrile complexes of  $[\text{V}(\text{PR}_3)_2(\text{N}^t\text{Bu})_2][\text{Al}(\text{PFTB})_4]$ , ( $\text{R} = \text{Me}, \text{Et}$ ) were prepared.  $[\text{V}(\text{PMe}_3)_2(\text{N}^t\text{Bu})_2][\text{Al}(\text{PFTB})_4]$ , ( $\text{PFTB} = \text{perfluoro-tert-butoxide}$ ) reacts with 2,6-xylylisocyanide ( $\text{CNXyl}$ ) or acetonitrile to afford complexes  $[\text{V}(\text{PMe})_2(\text{N}^t\text{Bu})_2(\text{CNXyl})][\text{Al}(\text{PFTB})_4]$  (**2**) and  $[\text{V}(\text{PMe})_2(\text{N}^t\text{Bu})_2(\text{MeCN})][\text{Al}(\text{PFTB})_4]$  (**3**). Complex **2** was crystallographically characterized, revealing a C–N bond length of (1.152(4) Å); the C–N stretching frequency occurs at  $2164 \text{ cm}^{-1}$  in the IR. To access the analogous carbon monoxide complex, the larger cone angle phosphine, triethylphosphine, was employed, starting from the chloride  $\text{VCl}(\text{PEt}_3)_2(\text{N}^t\text{Bu})_2$ , **4**, then to the lower coordinate  $C_{2v}$  symmetrical complex,  $[\text{V}(\text{PEt}_3)_2(\text{N}^t\text{Bu})_2][\text{Al}(\text{PFTB})_4]$ , **5**. Derivatization of **5** with DMAP (4-dimethylaminopyridine) afforded complex **6**,  $[\text{V}(\text{DMAP})(\text{PEt}_3)_2(\text{N}^t\text{Bu})_2][\text{Al}(\text{PFTB})_4]$ . Treatment of **5** with  $\text{CNXyl}$  yielded  $[\text{V}(\text{CNXyl})(\text{PEt}_3)_2(\text{N}^t\text{Bu})_2][\text{Al}(\text{PFTB})_4]$  (**7**) in 60% yield ( $\nu_{\text{C-N}} = 2156 \text{ cm}^{-1}$ ). The  $d^0$  vanadium bisimido, carbonyl complex,  $[\text{V}(\eta^1\text{-CO})(\text{PEt}_3)_2(\text{N}^t\text{Bu})_2][\text{Al}(\text{PFTB})_4]$  (**8**), was prepared via the exposure of **5** to 1 atm of CO. Complex **8** has a C–O stretching frequency of  $2015 \text{ cm}^{-1}$ . Isotopic labeling with 99%  $^{13}\text{C}$  reveals a stretching frequency of  $1970 \text{ cm}^{-1}$ , which confirms the assignment of the complex as a terminal  $\eta^1\text{-CO}$  complex. This is also implied by its NMR data in comparison to the other crystallographically characterized compounds presented here. The  $^{13}\text{C}\{^3\text{P}\}\{^1\text{H}\}$  NMR spectrum of  $^{13}\text{C}$  reveals a broad singlet at 228.36 ppm implying deshielding of the carbonyl carbon. This datum, in conjunction with the shielded vanadium NMR shift of  $-843.71 \text{ ppm}$ , suggests  $\pi$  back-bonding is operative in the bond between carbon monoxide and the  $d^0$  vanadium center in **8**. This model was further confirmed by density functional theory (DFT) analysis of the model complex  $[\text{V}(\eta^1\text{-CO})(\text{PMe}_3)_2(\text{N}^t\text{Bu})_2]^+$ , **9**, which reveals that the basis of the reduced stretching frequency in **8** is  $\pi$  back-bonding from the  $2b_1$  and  $1b_2$  orbitals of **8**.



## INTRODUCTION

There has been renewed interest in transition metal and actinide carbonyl complexes based both on fundamental coordination chemistry and their application in developing homogeneous alternatives to nonselective Fischer–Tropsch chemistry.<sup>1–14</sup> In particular,  $d^0$  transition metal carbonyl complexes have recently been shown to be important intermediates in two potentially industrially relevant transformations. Chirik and co-workers have characterized the complex  $((\text{Me}_2\text{Si}(\eta^5\text{-C}_5\text{Me}_4)(\eta^5\text{-C}_5\text{H}_3\text{-3-}^t\text{Bu})\text{Hf})_2(\mu\text{-NCO})\text{-CO})(\text{NCO})$  and have shown that the carbonyl ligand controls the regioselectivity in the products formed during the CO-induced cleavage of dinitrogen promoted by the *ansa*-hafnocene  $((\text{Me}_2\text{Si}(\eta^5\text{-C}_5\text{Me}_4)(\eta^5\text{-C}_5\text{H}_3\text{-3-}^t\text{Bu})\text{Hf})_2(\mu^2, \eta^2, \eta^2\text{-N}_2))$ .<sup>15,16</sup> Arnold and Bergman have also recently shown that the  $d^0$  carbonyl,  $(\text{BDI})\text{Nb}(\text{N}^t\text{Bu})(\eta^2\text{-MeCCPh})(\text{CO})$ , is a key intermediate in the (*Z*)-selective hydrogenation of alkynes to alkenes by  $(\text{BDI})\text{Nb}(\text{N}^t\text{Bu})(\text{CO})_2$  under an atmosphere of  $\text{H}_2/\text{CO}$ .<sup>17,18</sup> Remarkably this system yields exclusively products of hydrogenation and not hydroformylation.

Since the initial report of a Ti(IV) carbon monoxide complex in 1976 by Bigorne and co-workers,<sup>19</sup> a small group of formally  $d^0$  transition metal<sup>20–32</sup> (Table 1) and actinide carbonyl complexes<sup>33–35</sup> have been described. These complexes, both neutral and cationic, are intriguing from a coordination chemistry perspective because the nature of the bonding of the carbonyl ligand is not readily described by a simple model. Some of these complexes possess C–O stretching frequencies greater than free CO ( $\nu = 2143 \text{ cm}^{-1}$ ), which implies that  $\sigma$  bonding is the dominant interaction between the metal fragment and the carbonyl. This property has also been demonstrated for main group<sup>36–42</sup> and closed shell,  $d^8$  and  $d^{10}$  transition metal compounds.<sup>43–48</sup> Compounds possessing this property have been deemed “nonclassical” because, in contrast to the large number of  $d^{n \geq 0}$  transition metal carbonyls, the stretching frequency of the carbonyl ligand is not reduced via  $\pi$  to  $\pi^*$  back-bonding from the metal atomic orbitals to the

Received: September 21, 2012

Published: November 26, 2012

Table 1.  $d^0$  Group 4 and 5 Carbonyl Complexes

compound	C–O stretch in $\text{cm}^{-1}$	ref.
$(\text{Me}_2\text{Si}(\eta^5\text{-C}_5\text{Me}_4)(\eta^5\text{-C}_5\text{H}_3\text{-3-}^t\text{Bu})\text{Hf})_2(\mu\text{-NCO})(\text{CO})(\text{NCO})$	1959	15, 16
$(\text{BDI})\text{Nb}(\text{N}^t\text{Bu})(\eta^2\text{-RC}\equiv\text{CPh})(\text{CO})$	2052, R = Ph; 2039 R = Me	17, 18
$(\text{Cp}_2\text{Ti}(\text{CO}))_2(\mu\text{-}\eta^1\text{-C}_2(\text{CN})_4)$	2055	19
$[\text{TiCp}_2(\text{CO})_2][\text{BPh}_4]_2$	2119, 2099	20
$\text{Cp}^*_2\text{ZrH}_2(\text{CO})$	2044	21, 22
$\text{Cp}^*_2\text{HfH}_2(\text{CO})$	2036	23
$\text{Cp}_2\text{Zr}(\eta^2\text{-Me}_2\text{Si}=\text{N}^t\text{Bu})(\text{CO})$	1797	24
$\text{Cp}^*_2\text{Zr}(\eta^2\text{-E})(\text{CO})$	E = S, 2057; Se, 2037; Te, 2006	25
$\text{Cp}^*_2\text{Zr}(\text{Se})(\text{CO})$	2037	26
$[\text{Cp}_3\text{Zr}(\text{CO})][\text{BPh}_4]$	2150	27
$[\text{Cp}^*_2\text{Zr}(\eta^3\text{-C}_3\text{H}_3)(\text{CO})][\text{BPh}_4]$	2079	28
$[\text{Cp}_2\text{Zr}(\text{CH}(\text{Me})(6\text{-ethylpyrid-2-yl})(\text{CO}))][\text{BPh}_4]$	2095	29
$[(\text{C}_5\text{Me}_5)_2\text{Zr}(\eta^2\text{-COCH}_3)(\text{CO})][\text{CH}_3\text{B}(\text{C}_6\text{F}_5)_3]$	2105, 2152 (isomers)	30
$[\text{Cp}_2\text{Ta}(\text{CO})\text{H}_2][\text{PF}_6]$	2112	31
$\text{Cp}^*(\text{ArN}=\text{Ta})(\text{CO})[\text{Si}(\text{SiMe}_3)_3]\text{H}$	1986	32
$[\text{V}(\text{PEt})_2(\text{N}^t\text{Bu})_2(\text{CO})][\text{Al}(\text{PFTB})_4]$	2015	this work

carbonyl ligand lowest unoccupied molecular orbitals (LUMOs).

In this context, the formally  $d^0$  complexes that possess significantly reduced C–O stretching frequencies are of particular interest. These complexes do not possess electron density in a metal atomic orbital with which to back-bond with the carbonyl as would fit a classic Dewar–Chatt–Duncanson analysis of  $\pi$  back-bonding.<sup>49,50</sup> However, donation of electron density from  $\sigma$  M–E bonds (M = Ti, Zr, Hf, Nb, Ta; E = H, C, Si, O, S, Se, Te; Table 1) has been proposed as the primary means by which the metal fragment molecular orbitals (MO) participate in electron donation to the  $\pi^*$  orbitals of the carbonyl ligand (Figure 1).<sup>22,24,28</sup>

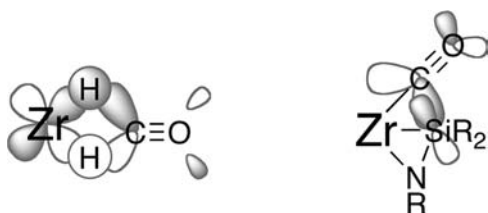


Figure 1. Two modes of  $\sigma$  to  $\pi^*$  donation in  $d^0$  carbonyls described previously. Zr =  $\text{Cp}_2\text{Zr}$  or  $\text{Cp}^*_2\text{Zr}$ ; Orbital interaction shown in the  $xy$  plane; see refs 22 and 24 for complete descriptions.

In contrast to this analysis, a recent theoretical study demonstrates that the bond between CO and  $(\text{Cp}')_3\text{U}$  ( $\text{Cp}' = \text{C}_5\text{H}_5, \text{C}_5\text{H}_4\text{TMS}, \text{C}_5\text{Me}_4\text{H}, \text{C}_5\text{Me}_5$ ) in  $(\text{Cp}')_3\text{U}(\text{CO})$  complexes involves back-bonding from the  $\text{Cp}'_3\text{U}$  ligand-based orbitals of  $\pi$  symmetry.<sup>9</sup> In other words, the partially filled, nonbonding f-orbitals do not significantly contribute to the reduction in the C–O stretching frequency. The extension of this model to  $d^0$  transition metal complexes does not necessarily hold. The complex  $[\text{Cp}_3\text{Zr}(\text{CO})][\text{BPh}_4]$  possesses a C–O stretching frequency of  $2150 \text{ cm}^{-1}$ .<sup>27</sup> Even when compared to the stretching frequency for  $\text{CO}^+$  ( $\nu = 2184 \text{ cm}^{-1}$ ),<sup>36,37</sup> there appears to be little to no back-bonding from the ligand-based orbitals of  $\pi$  symmetry. However, theoretical

analysis of the C–O stretching frequencies in  $(\text{Cp}')_3\text{U}$  clearly demonstrates the possibility of a similar interaction in transition metal complexes.<sup>32</sup>

We recently reported the (Z)-selective hydrogenation of alkynes to alkenes by  $[\text{V}(\text{PMe}_3)_3(\text{N}^t\text{Bu})_2][\text{Al}(\text{PFTB})_4]$ , **1**, (PFTB = perfluoro-*tert*-butoxide).<sup>51</sup> This complex is notable for several reasons including its “bent-metallocene like” electronic structure. This similarity derives from the nature of the donor orbitals of cyclopentadienes and imides, that is, both are  $1\sigma, 2\pi$  ligands.<sup>52–55</sup> This analogy between bent-metallocenes and bisimides has been noted previously.<sup>56–60</sup> Given the central role metallocenes have played in the development of organometallic chemistry,<sup>61–64</sup> some efforts have been made to access the frontier orbitals of bisimide systems to explore reactivity that is similar but not identical to that of the bent metallocenes.<sup>65</sup>

This previous work, however, has primarily focused on the heavier group 6 and 7 bisimides<sup>56,57</sup> and the activation of small molecule substrates by employing the  $d^0/d^2$  redox couple.<sup>66–71</sup> The  $\text{M}(\text{NR})_2$  fragment in these complexes is isolobal to the  $d^2$   $\text{Cp}_2\text{Hf}$  molecular fragment (Figure 2, Left), and suggests that  $d^2, 18 e^-, \text{Cp}_2\text{Ti}(\text{PMe}_3)_2$  is an apt model for their behavior.

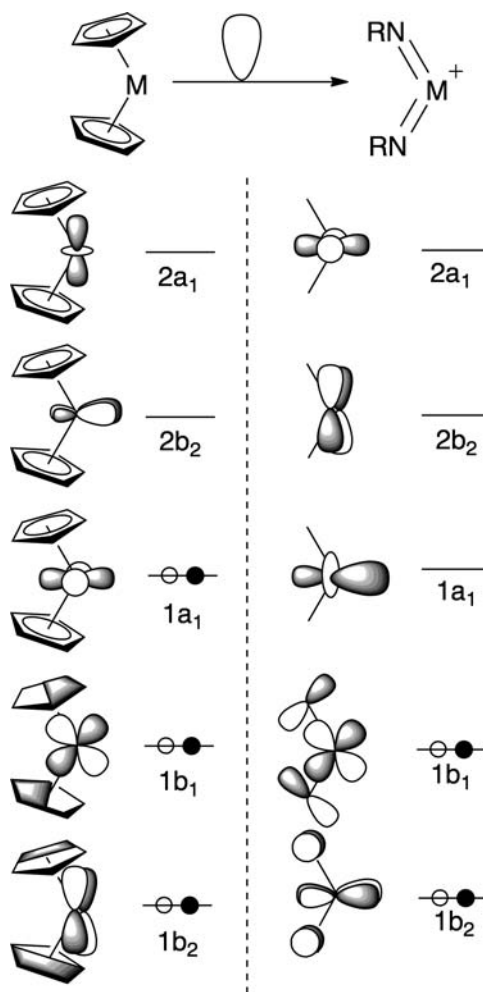
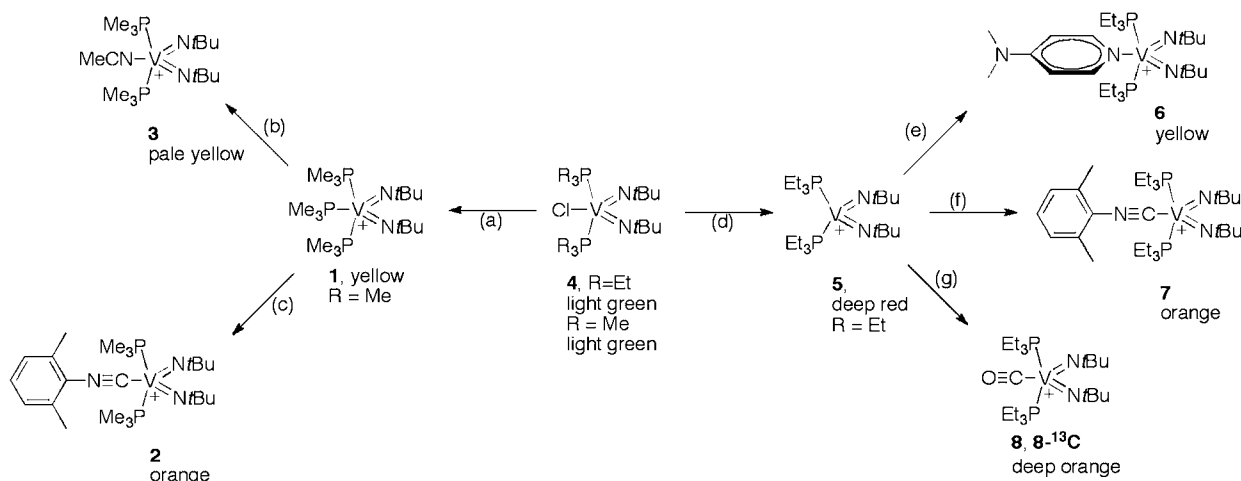


Figure 2. Illustration of the isolobal relationship between the frontier orbitals of  $\text{Cp}_2\text{M}$  and  $(\text{RN})_2\text{M}^+$  complexes. The given orbital occupation corresponds to a  $d^2$  electron configuration for the Group 4 metallocene and  $d^0$  for the cationic, group 5 bisimide, as Cps are monovalent and imides are divalent ligands.

Scheme 1<sup>a</sup>

<sup>a</sup>Conditions: (a) 3 equiv of  $\text{PMe}_3$ ; 1 equiv of  $\text{Li}[\text{Al}(\text{PFTB})_4]$ ,  $\text{PhCl}$ , 75%; see ref 51. for full details; (b) 5 equiv of  $\text{MeCN}$  in  $\text{PhCF}_3$ ; in situ characterization; (c) 1 equiv of  $\text{CNXyl}$ , diethyl ether, 58%; (d) 1 equiv of  $\text{Li}[\text{Al}(\text{PFTB})_4]$ ,  $\text{DCE}$ , 47%; (e) 1 equiv of  $\text{DMAP}$ ,  $\text{PhCF}_3$ , 50%; (f) 1 equiv of  $\text{CNXyl}$ ,  $\text{DCE}$ , 58%; (g) 1 atm  $\text{CO}$ , excess. The counteranion is  $[\text{Al}(\text{PFTB})_4]^-$  throughout.

Two seminal works have explored the reactivity of neutral  $d^0$  bisimides (V and Ta).<sup>72,73</sup> Both of these systems demonstrate remarkable  $\sigma$  C–H bond activation chemistry. However, these systems do not afford access to frontier MOs of the  $\text{M}(\text{NR})_2$  fragment as the covalently bonded, bulky silyl amide/imide ligands direct reactivity to the  $\pi$  orbitals of the individual imides.

We hypothesized that the use of labile supporting ligands and less sterically demanding imides as part of a cationic, group 5 complex would afford access to the frontier orbitals of the bent metallocene analogue and to the  $\sigma$  bond reactivity of these  $d^0$  bisimides.<sup>74–80</sup> A simple analysis of the bonding in the  $16 e^-$ ,  $[\text{V}(\text{PR}_3)_2(\text{N}^t\text{Bu})_2][\text{Al}(\text{PFTB})_4]$ , ( $\text{R} = \text{Me}, \text{Et}$ ) suggests that these compounds would be isolobal with  $\text{Cp}_2\text{Ti}(\text{PMe}_3)_2$ , but have a HOMO/LUMO gap shifted one set down (Figure 2, right). Given the remarkable hydrogenation chemistry observed for **1**, the nature of the bonding interactions of the complexes  $[\text{V}(\text{PR}_3)_2(\text{N}^t\text{Bu})_2][\text{Al}(\text{PFTB})_4]$  ( $\text{R} = \text{Me}, \text{Et}$ ) with alkynes and dihydrogen were of particular importance. Our interest in the bonding of  $d^0$  transition metal carbonyl complexes stems from the ability to use carbon monoxide as a spectroscopic probe to determine the nature of the frontier molecular orbitals in these bisimide complexes. Quantitative analysis of the molecular structure is not possible using substrates involved in the catalytic reaction because of several factors, including the complex spin system ( $\text{ABC}_2$ ; i.e. X (C or H), V, and P) in complexes of the type  $[\text{VL}(\text{PR}_3)_2(\text{N}^t\text{Bu})_2][\text{Al}(\text{PFTB})_4]$ , ( $\text{R} = \text{Me}, \text{Et}$ ,  $\text{L} = \text{H}_2$ , internal alkyne), high anisotropy of vanadium ( $I = 7/2$ ), weak bonding of the substrates of interest, the fluxional nature of the complexes, a narrow range of thermal stability, and a limited number of compatible solvents. Carbon monoxide, on the other hand, is the ideal  $\pi$  accepting ligand with which to study the electronic structure of these complexes because of its strong infrared signal and the ease of isotopic labeling.

Herein we report the synthesis and characterization of a series of nitrile, isocyanide, and carbon monoxide complexes of  $[\text{V}(\text{PR}_3)_2(\text{N}^t\text{Bu})_2][\text{Al}(\text{PFTB})_4]$  ( $\text{R} = \text{Me}, \text{Et}$ ). Structural, spectroscopic, and density functional theory (DFT) analyses demonstrate that the bond between  $[\text{V}(\text{PEt}_3)_2(\text{N}^t\text{Bu})_2][\text{Al}(\text{PFTB})_4]$  and  $\text{CO}$  involves back-bonding from the  $[\text{V}$

$(\text{PEt}_3)_2(\text{N}^t\text{Bu})_2$ ] ligand-based orbitals of  $\pi$  symmetry. Furthermore,  $[\text{V}(\text{PR}_3)_2(\text{N}^t\text{Bu})_2]^+$ , ( $\text{R} = \text{Me}, \text{Et}$ ) can act as both a  $\sigma$  acceptor and  $\pi$  donor in its binding of small molecule substrates.

## RESULTS AND DISCUSSION

**Synthesis of Isocyanide and Nitrile Complexes of  $[\text{V}(\text{PMe}_3)_2(\text{N}^t\text{Bu})_2][\text{Al}(\text{PFTB})_4]$ , **1**.** In the course of exploring the scope of the catalytic hydrogenation by **1**, isocyanides and nitriles were found to undergo exclusive ligand exchange with the equatorial  $\text{PMe}_3$ . Even in the presence of a 5-fold excess of substrate, no further exchange with the axial  $\text{PMe}_3$  ligands in **1** was observed (Scheme 1). While the equatorial phosphine readily dissociates at  $30^\circ\text{C}$ ,<sup>51</sup> the site selectivity of this exchange process suggests that there is a significant electronic contribution to the bonding in the newly formed complexes.

To explore the nature of bonding in these complexes, an isocyanide complex was synthesized on a preparative scale. The addition of a solution of 1 equiv of 2,6-xylylisocyanide ( $\text{CNXyl}$ ) in diethyl ether to a solution of **1** resulted in a rapid color change from yellow to orange. After workup,  $[\text{V}(\text{PMe}_3)_2(\text{N}^t\text{Bu})_2(\text{CNXyl})][\text{Al}(\text{PFTB})_4]$ , **2**, was isolated in 58% yield via crystallization from 1,2-dichloroethane ( $\text{DCE}$ ) (Scheme 1). The NMR characterization of this isolated complex matched that of the in situ prepared complex. In solution ( $\text{PhCF}_3$ ,  $\text{C}_6\text{D}_6$  insert) **2** presents both equivalent imido *tert*-butyl groups at 1.13 ppm and axial  $\text{PMe}_3$  ligands at 1.28 ppm ( $^2J_{\text{PH}} = 3.6$  Hz). The xylyl methyl groups are also equivalent with a single sharp singlet at 2.22 ppm. Most interestingly, the  $^{51}\text{V}$  NMR presents as a singlet at  $-930.21$  ppm ( $\Delta\nu_{1/2} = 159.88$  Hz), 138 ppm upfield from that of the starting complex, **1**, at  $-792.29$  ppm, implying that the vanadium nucleus is significantly more shielded. This upfield shift suggests that the isocyanide ligand is not acting solely as a  $\sigma$  donor, like  $\text{PMe}_3$  or  $\text{MeCN}$  ( $^{51}\text{V}$  NMR  $\delta -810.15$ ,  $\Delta\nu_{1/2} = 939.0$  Hz).

An X-ray crystallographic study confirmed the solution structural assignment. Complex **2** presents as distorted square base pyramid ( $\tau = 0.46$ , Figure 3, Left) with  $\text{C}_{2v}$  symmetry. This distortion from ideal  $\text{sp}$  geometry ( $\tau = 0.0$ )<sup>81,82</sup> reflects the



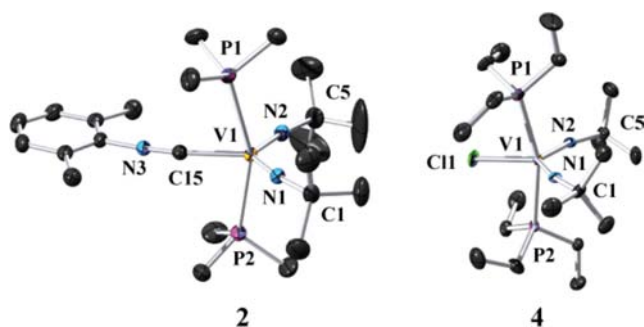


**Figure 3.** Molecular structures of **2** and **4**. Thermal ellipsoids are drawn at 50% probability level. Hydrogen atoms and counteranions ( $[\text{Al}(\text{PFTB})_4]^-$ ) have been removed for clarity. Selected bond lengths (Å) and angles (deg): Complex **2**–Left; N(1)–V(1), 1.690(3); N(2)–V(1), 1.679(3); C(15)–V(1), 2.152(4); C(15)–N(3), 1.152(4); N(2)–V(1)–N(1), 118.35(15); Complex **4**–Middle; N(1)–V(1), 1.687(4); N(2)–V(1), 1.681(4); N(2)–V(1)–N(1), 114.0(2).

still significant steric demands of the *tert*-butyl imido ligands on the relatively small vanadium nucleus (in comparison to Nb and Ta with either 2,6-diisopropylarylimido or *tris-tert*-butylsilylimido ligands).<sup>73,82</sup> As a result, the axial phosphines are displaced away from the imides as indicated by the N(1)–V(1)–P(2) and N(2)–V(1)–P(1) angles of 93.71(10)° and 97.96(11)°. The angle between the axial phosphines, 155.93(4)°, is about 5° greater than the corresponding angle in (py)<sub>2</sub>MeTa(NSi(*t*Bu)<sub>3</sub>)<sub>2</sub>, and about 5° smaller than that in (py)<sub>2</sub>MeTa(NAr)<sub>2</sub> (Ar = 2,6-diisopropyl),<sup>73,82</sup> which suggests that the combination of *tert*-butyl imides and vanadium is intermediate in terms of steric constraint in comparison to the much larger imides employed in the analogous V,<sup>72,83,84</sup> Nb,<sup>82</sup> and Ta<sup>73</sup> systems. However, such a comparison is purely qualitative because of the significantly greater V–P<sub>phosphine</sub> bond lengths (2.4526(10) and 2.4463(11) Å) in comparison to the Ta–N<sub>pyridine</sub> lengths (2.316(14) Å).

As high quality X-ray data sets for this series of cationic, vanadium bisimides are difficult to acquire on a routine basis because of the potential for extensive disorder in the S<sub>4</sub> symmetric anion,  $[\text{Al}(\text{PFTB})_4]^-$ ,<sup>51,85,86</sup> it is revealing to compare the metrical parameters of the bisimide core with the neutral precursor to **2**,  $\text{VCl}(\text{PMe}_3)_2(\text{N}^t\text{Bu})_2$ ,<sup>51</sup> and appropriate monoimido vanadium complexes (see the Supporting Information for a full ORTEP representation of the salt pair). As has been noted previously for other group 5 bisimides,<sup>73</sup> the angle N<sub>imide</sub>–V–N<sub>imide</sub> is less than the ideal of 120°. However, in contrast to its neutral precursor,  $\text{VCl}(\text{PMe}_3)_2(\text{N}^t\text{Bu})_2$ , (115.88(10)°) and the few other known neutral group 5 bisimides (115.3(7)° and 113.2(3)°),<sup>73,82</sup> it is expanded by about 5° to 118.35(15)°. This contraction of the angle between the imides in the neutral compounds, which is counter to the increased steric repulsion between the imide R groups, has been rationalized on the basis of electronic arguments. This rationalization of the observed trend in the neutral group 5 bisimides implies that the bisimides contribute less than 8e<sup>-</sup> to the metal (neutral ligand method). The expansion of the bisimide angle in the cation **2** could be driven by more effective donation of electron density to the metal center to compensate for the increased charge separation in the cation.

The imide bond lengths are nearly equivalent (1.690(3) and 1.679(3) Å). Surprisingly, they are about the same length as the

imides on the neutral precursor  $\text{VCl}(\text{PMe}_3)_2(\text{N}^t\text{Bu})_2$  (1.6888(19) and 1.6839(19) Å). These bond lengths in themselves are notable in that they are somewhat long in comparison to those of neutral vanadium monoimides such as  $\text{VCl}_3(\text{N}^t\text{Bu})$ ,<sup>87,88</sup> (1.616(9) Å), where bond lengths are consistent with triple bonding. The V=N–C angles in **2** and  $\text{VCl}(\text{PMe}_3)_2(\text{N}^t\text{Bu})_2$  are nearly equivalent and lie in the range of 167–169°. While these angles lie at the lower end of the range generally accepted to indicate linearity at an imide, they are smaller than their equivalent angles on group 5 aryl and silyl bisimides (cf. 176.3(10) and 168.1(8)°; TaNSiR<sub>3</sub><sup>73</sup> and 170.9(5) and 165.4(5)°; TaNAr).<sup>82</sup> These silyl and aryl bisimides can participate in either N(pπ)⇒Si(pσ\*) or N–(pπ)⇒Ar(pπ\*) interactions that lead to linearization of the M=N–X angle (X = C or Si). This geometric difference suggests that **2** and  $\text{VCl}(\text{PMe}_3)_2(\text{N}^t\text{Bu})_2$ , with alkyl imides, have greater electron density localized at nitrogen and a larger contribution of sp<sup>2</sup> hybridization. The main difference between **2** and its neutral precursor is the slight contraction of the V–P bond lengths from 2.4507(7) and 2.4546(7) Å to 2.4526(10) and 2.4463(11) Å.

In the context of defining the bonding of π accepting ligands to  $[\text{V}(\text{PR}_3)_2(\text{N}^t\text{Bu})_2]^+$ , the geometric parameters of the isocyanide ligand, like the NMR data for **2**, indicate some degree of π back-bonding from the complex. The isocyanide ligand is essentially coplanar with the N<sub>imide</sub>–V–N<sub>imide</sub> plane, and it is centrally located in the bisimide wedge, equidistant from the imides and phosphines. The V–C–N angle is near linear, 173.9(3)°. The V–C bond length is 2.152(4) Å and the C–N bond length is 1.152(4) Å. Crystallographically characterized vanadium CNXyl complexes are rare. The nearest point of comparison is the V(III) (PNP<sup>ipr</sup>)VTe(CNXyl)<sub>2</sub> (PNP<sup>ipr</sup> = N(2-PiPr<sub>2</sub>-4-methylphenyl)<sub>2</sub>), which possess two crystallographically equivalent isocyanides with a V–C bond of 2.050 Å and a C–N bond of 1.155 Å.<sup>89</sup> As **2** exhibits a C–N stretching frequency of 2164 cm<sup>-1</sup>, and (PNP<sup>ipr</sup>)VTe(CNXyl)<sub>2</sub> has stretching frequencies of 2022 and 2002 cm<sup>-1</sup> (Free CNXyl = 2116 cm<sup>-1</sup>, Table 2),<sup>90</sup> it is clear that the C–N bond length is

**Table 2.** Reference CNXyl Stretching Frequencies and C–N Bond Lengths

compound	C–N bond length, Å	C–N stretching frequency, cm <sup>-1</sup>	ref.
CNXyl	1.160(3)	2116	90
$[\text{V}(\text{PMe}_3)_2(\text{N}^t\text{Bu})_2(\text{CNXyl})]^+$	1.152(4)	2164	this work
$[\text{V}(\text{PEt}_3)_2(\text{N}^t\text{Bu})_2(\text{CNXyl})]^+$	N/A	2156	this work
(PNP <sup>ipr</sup> )VTe(CNXyl) <sub>2</sub>	1.155	2022, 2002	89
$[\text{Ti}(\text{CNXyl})\text{Cl}_4]_2$	1.147(8)	2210	92
$\text{CpTiI}_2(\text{CNXyl})_2$	1.154(4)	2156	93
$[\text{Cp}_2\text{Hf}(\text{CNXyl})(\eta^2\text{-RCNR}')^+]$	N/A	2189	94

not always an accurate measure of back-bonding. In comparing these two complexes, the V–C bond length correlates best with the observed IR stretching frequencies, and, as the absorption for **2** is slightly blue-shifted from that of free CNXyl, might initially suggest an absence of π back-bonding.

However, a clear trend can be delineated by examining the d<sup>0</sup> and d<sup>1</sup> Group 4, CNXyl complexes. Two factors make analysis of π back-bonding via isocyanide C–N bond lengths and stretching frequencies complex: (1) In isocyanides, the C lone pair is more antibonding with respect to the C–N bond (versus

in CO where it is nonbonding with respect to the C–O bond). Therefore donation of the lone pair to the metal actually raises the C–N stretching frequency and leads to shortened C–N bond lengths in the solid state.<sup>91</sup> (2) As with carbon monoxide, the C–N stretching frequency is higher in cationic complexes. With these constraints in mind, it is of interest to compare free CNXyl with a C–N bond length of 1.160(3) Å and a C–N stretching frequency of 2116 cm<sup>-1</sup> with the d<sup>0</sup>, Ti(IV) complex, [Ti(CNXyl)Cl<sub>4</sub>]<sub>2</sub>, which has a C–N distance of 1.147(8) Å and an IR absorption at 2210 cm<sup>-1</sup> (Table 2).<sup>92</sup> This pair of data implies that in the complex [Ti(CNXyl)Cl<sub>4</sub>]<sub>2</sub>, CNXyl can be thought of as very nearly a solely  $\sigma$  donor. Therefore the bonding in **2** must be considered to contain some component of  $\pi$  back-bonding from [V(PR<sub>3</sub>)<sub>2</sub>(N<sup>t</sup>Bu)<sub>2</sub>]<sup>+</sup>. The d<sup>1</sup> Ti(III) complex, CpTiI<sub>2</sub>(CNXyl)<sub>2</sub>, possesses similar metrics to those of **2** (1.154(4) Å and C–N absorption at 2156 cm<sup>-1</sup>).<sup>93</sup> The authors propose that this complex, in comparison to [Ti(CNXyl)Cl<sub>4</sub>]<sub>2</sub>, possesses  $\pi$  back-bonding along the classical Dewar–Chatt–Duncanson model. The sole other reported cationic, d<sup>0</sup> CNXyl complex, [Cp<sub>2</sub>Hf(CNXyl)( $\eta^2$ -RCNXyl)]-[B(Ph)<sub>4</sub>] (R = CCMe), has an isocyanide C–N absorption at 2189 cm<sup>-1</sup>.<sup>94</sup> As the C–N absorption of complex **2** lies 25 cm<sup>-1</sup> lower than [Cp<sub>2</sub>Hf(CNXyl)( $\eta^2$ -RCNR')][B(Ph)<sub>4</sub>], the V–C bond in **2** must contain some component of  $\pi$  back-bonding.

**Synthesis and Characterization of [V(PET<sub>3</sub>)<sub>2</sub>(N<sup>t</sup>Bu)<sub>2</sub>]-[Al(PFTB)<sub>4</sub>].** With this initial information about the bonding in **2**, we sought less ambiguous confirmation of the hypothesis that [V(PR<sub>3</sub>)<sub>2</sub>(N<sup>t</sup>Bu)<sub>2</sub>]<sup>+</sup> (R = Me, Et) can act as both a  $\sigma$  acceptor and  $\pi$  donor in its binding of small molecule substrates. Since [V(PMe<sub>3</sub>)<sub>3</sub>(N<sup>t</sup>Bu)<sub>2</sub>][Al(PFTB)<sub>4</sub>] undergoes a dramatic transformation with carbon monoxide, access to a stable, four-coordinate bisimide cation was sought to avoid reactivity derived from equatorial ligand exchange. To this end, use of the larger cone angle PET<sub>3</sub> (132° vs 118° for PMe<sub>3</sub>)<sup>95</sup> afforded the desired cation via a synthetic route analogous to the one for [V(PMe<sub>3</sub>)<sub>3</sub>(N<sup>t</sup>Bu)<sub>2</sub>][Al(PFTB)<sub>4</sub>]. The bisimido vanadium chloride supported by PET<sub>3</sub>, **4**, was prepared by the addition of 2.1 equiv of PET<sub>3</sub> to VCl<sub>2</sub>(N<sup>t</sup>Bu)(NTMS(<sup>t</sup>Bu)) in toluene. After heating the reaction mixture at reflux for 16 h, workup, and crystallization from HMDSO, **4** was obtained in good yield (83%, Scheme 1). Complex **4** has NMR spectroscopic characteristics similar to those of its previously reported PMe<sub>3</sub> analogue including a <sup>51</sup>V NMR shift of  $\delta$  -757.33 ppm. The connectivity was confirmed by an X-ray diffraction (XRD) study (Figure 3, middle). The key features of the structure (Figure 3) are essentially invariant from those of the PMe<sub>3</sub> analogue,<sup>51</sup> which was reviewed above as a comparison to the isocyanide cation **2**. The only distinguishing features are longer V–P bonds (2.4999(14) and 2.5006(14) Å compared to 2.4507(7) and 2.4546(7) Å), a slightly more linear P–V–P angle, and a reduced N–V–N angle, giving a  $\tau$  = 0.60 compared to a  $\tau$  = 0.65 for the PMe<sub>3</sub> analogue.

The four coordinate, cationic vanadium bisimide was then prepared by the addition of a DCE solution of **4** to a slurry of Li[Al(PFTB)<sub>4</sub>] in DCE at room temperature. This addition resulted in a shift in color from light green to a very deep red. While this complex is generated quantitatively on mixing in several solvents (*d*<sub>2</sub>-DCM, DCE, PhCF<sub>3</sub>), reasonable preparative yields (ca. 40–60%) could only be obtained by crystallization from DCE as red blades. Complex **5** prepared by this method can be used directly within hours, but storage at -40 °C in the solid state under N<sub>2</sub> leads to about 10% loss per week. In comparison to the chloride precursor, **5** has a <sup>51</sup>V

NMR resonance of  $\delta$  -278.99 ppm ( $\Delta\nu_{1/2}$  = 80.78 Hz, in PhCF<sub>3</sub> (C<sub>6</sub>D<sub>6</sub> insert)). Like all the complexes presented here, the <sup>31</sup>P NMR is largely uninformative as unresolved V–P coupling gives broad peaks: **5** has a single <sup>31</sup>P resonance at  $\delta$  26.69 ppm ( $\Delta\nu_{1/2}$  = 2674.50 Hz, in PhCF<sub>3</sub> (C<sub>6</sub>D<sub>6</sub> insert)).

As all attempts to obtain a crystal structure of **5** were unsuccessful, we sought to derivatize **5** to confirm NMR assignments and molecular geometry. This goal was achieved by generating **5** in the presence of DMAP in PhCF<sub>3</sub>. After workup the desired complex, **6**, was obtained in 50% yield by crystallization from PhCF<sub>3</sub> (Scheme 1) as yellow blocks. The NMR spectroscopic characteristics of this complex are very similar to those for **1** and **3**. The <sup>51</sup>V NMR resonance is shifted from **5** at  $\delta$  -278.99 ppm to  $\delta$  -728.16 similar to that observed for **1** (-792.29 ppm). The <sup>1</sup>H and <sup>31</sup>P NMR spectra of **6** are similar to those observed for **3**. The molecular structure was confirmed by XRD study. This complex, like many complexes supported by the [Al(PFTB)<sub>4</sub>]<sup>-</sup> anion, suffered from significant disorder in the anion. Nonetheless, the molecular geometry was confirmed demonstrating that the four-coordinate cation is successfully generated.

**Isocyanide and Carbon Monoxide Complexes of [V(PET<sub>3</sub>)<sub>2</sub>(N<sup>t</sup>Bu)<sub>2</sub>][Al(PFTB)<sub>4</sub>].** Treatment of a DCE solution of freshly prepared **5** with a solution of CNXyl in DCE resulted in a rapid color change from deep red to orange. Stirring the reaction mixture overnight resulted in no further observable reactivity and it afforded, after appropriate workup, complex **7** in 60% yield as orange blades (Scheme 1). Several attempts to obtain an XRD structure failed to yield resolution sufficient to obtain connectivity, but solution NMR studies confirmed a structure analogous to **3** with equivalent *tert*-butyl imido groups and PET<sub>3</sub> ligands. Most notably, the vanadium NMR shift is essentially unchanged from that of the PMe<sub>3</sub> analogue **3** at  $\delta$  -903.43 ppm (compared with -930.21 ppm). This similarity in bonding structure is mirrored in the IR spectrum of **7** in which the C–N stretch is located at 2156 cm<sup>-1</sup> (Table 2), very nearly identical to that of **3** at 2164 cm<sup>-1</sup>. This pattern suggests that bonding of the isocyanide is unperturbed by the nature of the phosphine and that any  $\pi$  back-bonding is independent of the V–P  $\sigma$  bonds, as the C–N stretching frequency is largely independent of the identity of the supporting phosphine ligand.

The carbonyl complex was most readily prepared by the addition of 1 atm of CO to a degassed solution of **5** in PhCF<sub>3</sub> or *d*<sub>4</sub>-DCE in a J. Young NMR tube. Within 5 min the color shifted from deep red to deep orange, and examination by NMR revealed complete conversion to the desired product **8** (Scheme 1). While **8** can be isolated on a preparative scale, it decomposed before satisfactory elemental analysis could be obtained. Likewise, crystallographic analysis proved troublesome: when single crystals were placed on a slide in Paratone-N oil under a lamp they rapidly evolved a gas, presumably CO, and immediate interrogation via X-ray led to sudden crystal decay.

The *tert*-butyl imido groups of **8** are equivalent in solution as are the supporting triethyl phosphine ligands, similar to its isocyanide congener **7**. The <sup>51</sup>V NMR presents as a pseudo doublet at  $\delta$  -843.71 ppm (<sup>1</sup>J<sub>VP</sub> = 225.13 Hz), which is significantly shielded in comparison to the four coordinate precursor **5**, although not quite as shielded as the two isocyanide complexes (Figure 4). This upfield shift suggests that carbon monoxide, like isocyanide, is not acting solely as a  $\sigma$  donor. The pseudo doublet of **8** in the <sup>51</sup>V NMR spectrum is unusual. Since **8**-<sup>13</sup>C presents as a broad singlet at -845.06

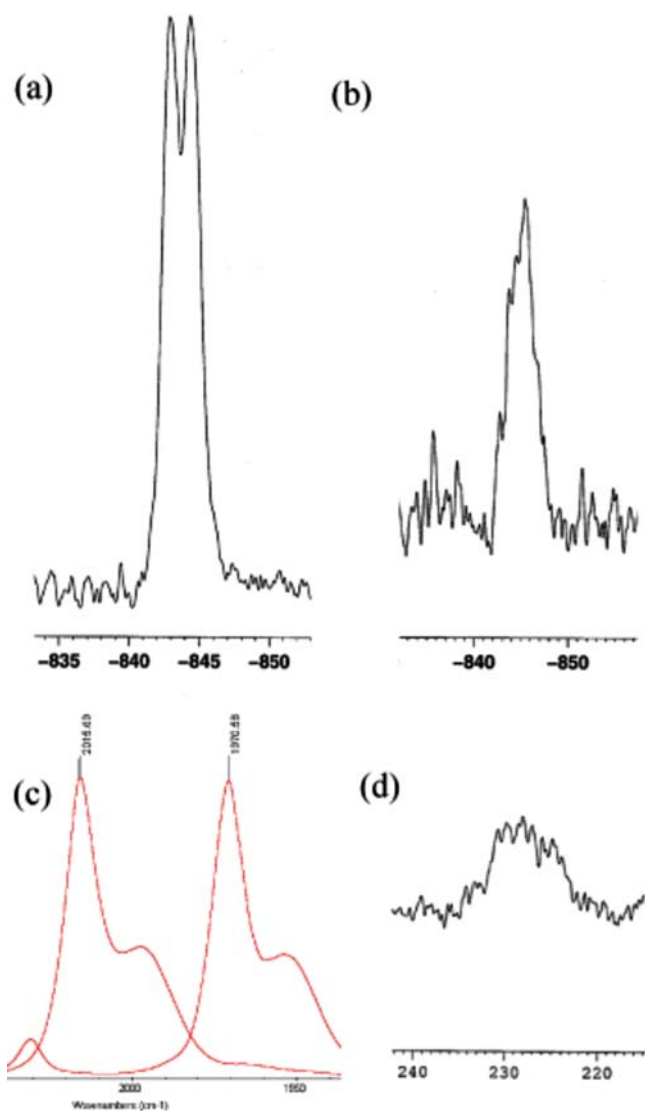


**Figure 4.** (a)  $^{51}\text{V}$  NMR of **8**. (b)  $^{51}\text{V}$  NMR of  $8\text{-}^{13}\text{C}$ . (c) Solution IR of **8** and  $8\text{-}^{13}\text{C}$ . (d)  $^{13}\text{C}\{^{31}\text{P}\}\{^1\text{H}\}$  NMR spectrum of  $8\text{-}^{13}\text{C}$ .

ppm ( $\Delta\nu_{1/2} = 531.05$  Hz), the observed coupling constant is not due to V–C coupling. Rather it is the result of V–P coupling. This phenomenon is similar to that observed for metal complexes containing two equivalent  $\text{PMe}_3$  ligands. The proton resonance for the  $\text{PMe}_3$  ligands in these systems shows a pseudo triplet in the extreme where  $J_{\text{PP}}$  is greater than  $J_{\text{HP}}$ . The equivalent scenario for  $^{51}\text{V}$  NMR was reported by us for the *bis*- $\text{PMe}_3$  complex,  $[\text{VCl}(\text{PMe}_3)_2(\text{N}^t\text{Bu})(\text{NH}^t\text{Bu})][\text{Al}(\text{PFTB})_4]$ , which presents unresolved pseudo triplets in its  $^{51}\text{V}$  spectra: that is,  $J_{\text{PP}}$  is larger than  $J_{\text{VP}}$ .<sup>51</sup> In the case of **8**, the opposite is true:  $J_{\text{VP}}$  is larger than  $J_{\text{PP}}$ , leading to the observed “Batman” pseudo doublet. It is tempting in the context of the larger argument—that CO binds via  $\pi$  back-bonding with filled vanadium bisimido orbitals of  $\pi$  symmetry—to ascribe the observation of this coupling constant to the decreased local anisotropy at vanadium because of increased local symmetry via the formation of the  $\pi$  bonds. It should be noted that among the five-coordinate bisphosphine, bisimido complexes presented here and previously, those containing a  $\pi$  accepting axial ligand generally present  $^{51}\text{V}$  resonances with a smaller  $\Delta\nu_{1/2}$ .

These NMR data, which imply a  $\pi$  interaction, are supported by examining the solution infrared spectrum of **8** which shows a

strong C–O absorption at  $2015\text{ cm}^{-1}$ . Upon labeling with  $^{13}\text{C}$  this absorption shifts to  $1970\text{ cm}^{-1}$ , as is expected by the simple harmonic oscillator model and confirms the species as a terminal, (i.e.,  $\eta^1$ ) CO complex (Figure 4). The  $^{13}\text{C}\{^{31}\text{P}\}\{^1\text{H}\}$  NMR spectrum of  $8\text{-}^{13}\text{C}$  gives a very broad resonance due to unresolved V–C coupling at  $228.36$  ppm (Figure 3). This resonance is shifted downfield of that of free CO ( $181.83$  ppm in  $\text{PhCF}_3$ ) by  $46.56$  ppm, which demonstrates donation of electron density into the  $\pi^*$  orbitals of the CO ligand (Figure 4). Sigma-only complexes present  $^{13}\text{C}$  shifts upfield of free CO. Taken together, these experimental data strongly supports the hypothesis that the carbonyl and isocyanide ligands participate in  $\pi$  back-bonding with  $[\text{V}(\text{PR}_3)_2(\text{N}^t\text{Bu})_2]^+$  and that reduction in C–O stretching frequency is *not* due solely to a  $\sigma$  to  $\pi^*$  interaction, as has been proposed to be the dominant electronic interaction in other  $d^0$  carbonyl complexes.

**Computational Studies and the Electronic Structure of  $[\text{V}(\eta^1\text{-CO})(\text{PR}_3)_2(\text{N}^t\text{Bu})_2]^+$ .** To gain further understanding of the bonding in the carbonyl complex and to confirm the hypothesis that the V–C bond involves  $\pi$  back-bonding from the  $[\text{V}(\text{PET}_3)_2(\text{N}^t\text{Bu})_2]^+$  ligand-based orbitals of  $\pi$  symmetry, DFT calculations were performed on the model complex  $[\text{V}(\eta^1\text{-CO})(\text{PMe}_3)_2(\text{N}^t\text{Bu})_2]^+$ , **9**, (B3LYP, see Experimental Section and Supporting Information). The geometry optimized structure of **9** reveals overall  $C_{2v}$  symmetry in accord with the solution-state symmetry observed by NMR for complex **8** and the solution and solid-state symmetry observed for **2** (Figure 5). The geometry of **9** is best approximated as a distorted

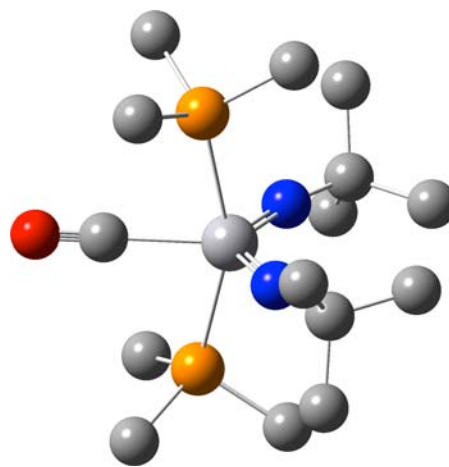


**Figure 5.** Geometry-optimized (B3LYP) coordinates of **9**. The hydrogen atoms were omitted for clarity. Selected bond lengths (Å) and angles (deg): V– $\text{N}_{\text{imido}}$ , 1.671; V– $\text{C}_{\text{CO}}$ , 2.112; C–O, 1.141;  $\text{N}_{\text{imido}}\text{–V–N}_{\text{imido}}$ , 118.35.

trigonal bipyramid with  $\tau = 0.60$  (Figure 5). The  $\text{N}_{\text{imido}}\text{–V–N}_{\text{imido}}$  bond angle is  $118.4^\circ$ ; the V– $\text{N}_{\text{imido}}$  distances are both  $1.67$  Å; and the V– $\text{N}_{\text{imido}}\text{–C}$  angles are both  $168^\circ$  in good agreement with the parameters observed for the isocyanide complex **2**.

The frontier orbitals of **9** were then compared with fragment orbitals of  $[\text{V}(\text{PMe}_3)_2(\text{N}^t\text{Bu})_2]^+$  and CO. The fragment analysis was performed using the coordinates generated by the geometry optimization on **9**. This analysis is the basis of the molecular orbital correlation diagram presented in Figure 6. The key features of this diagram and the molecular orbital plots are the interactions of the  $1b_1$ ,  $2b_1$ , and  $1b_2$  orbitals of the  $[\text{V}(\text{PMe}_3)_2(\text{N}^t\text{Bu})_2]^+$  with the  $\pi^*$  of CO. This is clearly seen in



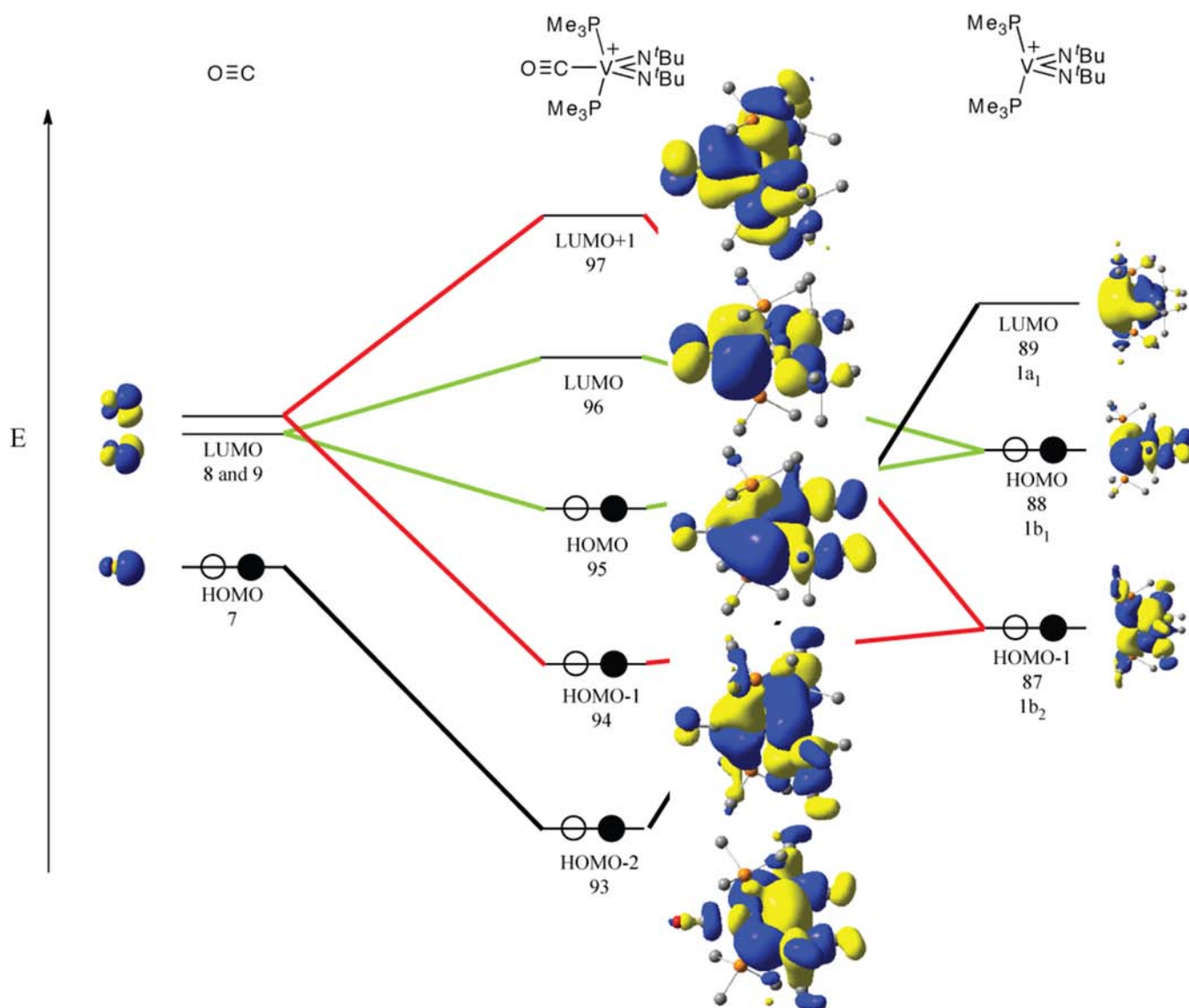


**Figure 6.** DFT MO correlation diagram of  $[\text{V}(\text{PMe}_3)_2(\text{N}^t\text{Bu})_2]^+$  and CO in the bonding of **9**. Relative energies and overlap are not to scale. Green lines show in-plane  $\pi$  interactions, red lines show out of plane interactions, black lines show  $\sigma$  interactions.

the interaction of in plane  $\pi^*$  orbital of CO (plane as defined by  $\text{N}_{\text{imide}}-\text{V}-\text{N}_{\text{imide}}$ ) with the  $1b_2$  orbital of  $[\text{V}(\text{PMe}_3)_2(\text{N}^t\text{Bu})_2]^+$  (HOMO (88)), which gives rise to the HOMO (95) and LUMO (96) of the complex (Green lines, Figure 6). The out of plane  $\pi^*$  orbital of CO interacts with the linear combination of the  $1b_1$  and  $2b_1$  (HOMO-4 (84) and HOMO-1 (87)) orbitals of the  $[\text{V}(\text{PMe}_3)_2(\text{N}^t\text{Bu})_2]^+$ , which gives rise to two molecular orbitals LUMO+1 (97) and HOMO-1 (94) (Red lines, Figure 6). This interaction is more complex and implicates the previously proposed  $\sigma$  to  $\pi^*$  interaction is a component of the  $\pi$  back-bonding (See Supporting Information for full MO diagram).

## CONCLUSIONS

A series of carbon monoxide, isocyanide, and nitrile complexes of cationic, vanadium bisimides were prepared. In the case of the more strongly  $\sigma$  donating isocyanide or nitrile ligands, this synthesis was most conveniently achieved by the displacement of  $\text{PMe}_3$  from  $[\text{V}(\text{PMe}_3)_3(\text{N}^t\text{Bu})_2][\text{Al}(\text{PFTB})_4]$ . However, in the case of carbon monoxide the use of a four coordinate

precursor,  $[\text{V}(\text{PEt}_3)_2(\text{N}^t\text{Bu})_2][\text{Al}(\text{PFTB})_4]$ , was necessary to isolate the desired complex. The formation of the requisite  $[\text{V}(\text{PEt}_3)_2(\text{N}^t\text{Bu})_2][\text{Al}(\text{PFTB})_4]$  was confirmed via derivatization with DMAP and CNXyl. The examination of these complexes implicates the role of  $\pi$  back-bonding from the formally  $d^0$  vanadium complex in binding  $\pi$  accepting ligands.

The bonding model developed here for the lowered C–O stretching frequency in **8** is distinctly different from that used to account for the lowered C–O stretching frequency in most d-transition metal complexes. In this present case, the electron density originates from the  $d$   $\pi$  symmetry orbitals that are RN–V bonding. This mode of weak bonding of  $\pi$  accepting ligands provides the basis to understand the bonding and hence activation barriers of small molecules to  $d^0$  transition metal complexes. Wolczanski, Chirik, and Andersen have indirectly implicated similar  $d^0$  imide/Cp and bisimide complexes in the formation of intermediate  $\sigma$   $\text{H}_2$  and C–H complexes via KIE and EXSY experiments, as well as DFT calculations.<sup>96–99</sup> The results presented here suggest that these reaction intermediates may be formed not just on the basis of a simple Lewis acid/base

pair, but may also involve  $\pi$  back-bonding. Ongoing work focuses on applying the understanding of the molecular orbital structure of these unusual complexes to the design of other novel catalytic reactions and the direct observation of reaction intermediates.

## EXPERIMENTAL SECTION

**General Details.** Unless otherwise noted, all reactions were performed using standard Schlenk line techniques or in an MBraun inert atmosphere box under an atmosphere of argon or dinitrogen (<1 ppm  $O_2/H_2O$ ), respectively. All glassware and cannulae were stored in an oven at about 425 K. Pentane, diethyl ether, tetrahydrofuran, 1,2-dimethoxyethane, dichloromethane, and toluene were purified by passage through a column of activated alumina and degassed prior to use. HMDSO was distilled from sodium/benzophenone, degassed by bubbling argon through the liquid for 15 min, and stored over 4 Å sieves. Acetonitrile was distilled from  $P_2O_5$  and degassed by bubbling argon through the liquid for 15 min.  $C_6D_6$  was vacuum-transferred from sodium/benzophenone and degassed with three freeze–pump–thaw cycles.  $1,2-C_2D_4Cl_2$  was vacuum transferred from  $CaH_2$  and degassed with three freeze–pump–thaw cycles. NMR spectra were recorded on Bruker AV-300, AVB-400, AVQ-400, AV-500, and AV-600 spectrometers.  $^1H$  and  $^{13}C\{^1H\}$  chemical shifts are given relative to residual solvent peaks.  $^{31}P$ ,  $^{51}V$ ,  $^{19}F$ , and  $^{27}Al$  chemical shifts were referenced to external standards ( $P(OMe)_3$  at 1.67 ppm,  $VOCl_3$  at 0.00 ppm,  $CFCl_3$  at 0.00 ppm, and 1 M  $Al(NO_3)_3$  in  $H_2O/D_2O$  at 0 ppm, respectively). Proton and carbon NMR assignments were routinely confirmed by  $^1H$ – $^1H$  (COSY) or  $^1H$ – $^{13}C$  (HSQC and HMBC) experiments as necessary.  $^{13}C$  resonances marked with \* are observed only by HMBC. Infrared (IR) samples were prepared as Nujol mulls and were taken between KBr disks on a Thermo Scientific iS10 FT-IR spectrometer except where noted in text. The following chemicals were purified prior to use: 1,2-dichloroethane was distilled from  $CaH_2$  and was degassed by bubbling argon through the liquid for 15 min and  $\alpha$ ,  $\alpha'$ ,  $\alpha'$ -trifluorotoluene ( $PhCF_3$ ), was distilled from  $P_2O_5$  and degassed by bubbling argon through the liquid for 15 min.  $Li[Al(PFTB)_4]$ ,<sup>85</sup>  $VCl_2(N^tBu)(NTMS^tBu)$ ,<sup>51</sup> and  $[V(PMe_3)_3(N^tBu)_2][Al(PFTB)_4]$ <sup>51</sup> were prepared using literature procedures. All other reagents were acquired from commercial sources and used as received. Elemental analyses were determined at the College of Chemistry, University of California, Berkeley. The X-ray structural determinations were performed at CHEXRAY, University of California, Berkeley, on Bruker SMART 1000, SMART APEX, or MicroSTAR-H X8 APEXII diffractometers.

**Preparation of  $[V(PMe_3)_2(N^tBu)_2(CNXYl)][Al(PFTB)_4]$  (2).** To a solution of **1** (777 mg, 0.56 mmol) in 15 mL of diethyl ether was added 2,6-xylylisocyanide (1 equiv, 75 mg, 0.56 mmol) in 10 mL of diethyl ether via cannula. After this addition, the reaction mixture was stirred for 12 h. The reaction mixture was then reduced to a residue in vacuo and extracted with 1,2-dichloroethane, filtered via cannula, and reduced until the product began to crystallize. After cooling the solution to  $-15^\circ C$  overnight, the product was obtained in 58% yield (467 mg) after decantation, as yellow-orange blocks. Subsequent recrystallization from DCE at  $-15^\circ C$  afforded X-ray quality crystals.  $^1H$  NMR ( $PhCF_3$  ( $C_6D_6$  insert), 600.1 MHz)  $\delta$  2.22 (s, *ortho*-ArMe, 6H), 1.28 (pseudo t, axial  $PMe_3$ , 18H,  $^2J_{PH} = 3.6$  Hz), 1.13 (s, *NtBu*, 18H). Aryl proton resonances could not be observed because of overlapping *protio*-solvent resonances.  $^{13}C$  NMR ( $PhCF_3$  ( $C_6D_6$  insert), 150.9 MHz)  $\delta$  135.09 (s, Ar), 131.12 (q,  $C(CF_3)_3$ ,  $^1J_{CF} = 41.35$  Hz), 69.5\* ( $\alpha$ -*NtBu*), 33.17 (t,  $\beta$ -*NtBu*,  $^3J_{PC} = 3.32$  Hz), 18.01 (s, Ar-*ortho*-Me), 17.40 (d,  $PMe_3$ ,  $^1J_{PC} = 14.34$  Hz), 17.33 (d,  $PMe_3$ ,  $^1J_{PC} = 14.34$  Hz). The  $\alpha$ - $C(CF_3)_3$  resonance and three Ar carbons could not be observed.  $^{31}P\{^1H\}$  NMR ( $PhCF_3$  ( $C_6D_6$  insert), 242.9 MHz)  $\delta$  2.61 (vbr s,  $\Delta\nu_{1/2} = 2056.60$  Hz).  $^{51}V\{^1H\}$  NMR ( $PhCF_3$  ( $C_6D_6$  insert), 157.7 MHz)  $\delta$  -930.21 (br s,  $\Delta\nu_{1/2} = 159.88$  Hz).  $^{19}F$  NMR ( $PhCF_3$  ( $C_6D_6$  insert), 376.5 MHz)  $\delta$  -74.55 (s).  $^{27}Al$  NMR ( $PhCF_3$  ( $C_6D_6$  insert), 104.3 MHz)  $\delta$  34.74 (s,  $\Delta\nu_{1/2} = 3.18$  Hz). Anal. Calcd (%) for  $C_{40}H_{49}AlF_{36}N_3O_4P_2V$ : C, 32.91; H, 3.38; N, 2.88. Found: C, 32.67; H, 3.10; N, 2.84. IR (KBr,  $cm^{-1}$ ): 2164 (s), 1352 (s),

1172 (s), 1110 (w), 945 (s), 831 (m), 755 (w), 601 (w), 560 (w), 537 (w), 446 (s). Mp = 185–187  $^\circ C$  (dec.).

**Observation of  $[V(PMe_3)_2(N^tBu)_2(MeCN)][Al(PFTB)_4]$  (3).** A J. Young NMR tube was charged with  $[V(PMe_3)_3(N^tBu)_2][Al(PFTB)_4]$  (34.7 mg, 0.025 mmol),  $\sim 0.7$  mL of  $PhCF_3$ , MeCN (5 equiv, 7  $\mu L$ , 0.13 mmol) and a sealed capillary filled with  $C_6D_6$ . On mixing, the solution shifted from yellow to pale yellow, nearly colorless.  $^1H$  NMR ( $PhCF_3$  ( $C_6D_6$  insert), 600.1 MHz)  $\delta$  1.50 (br s, free MeCN), 1.28 (br s, equatorial MeCN, 1.5H), 1.25 (d, axial  $PMe_3$ , 18H,  $^2J_{PH} = 7.8$  Hz), 1.12 (s, *NtBu*, 18H), 0.78 (br s, free  $PMe_3$ , 9H).  $^{13}C$  NMR ( $PhCF_3$  ( $C_6D_6$  insert), 150.9 MHz)  $\delta$  131.11 (q,  $C(CF_3)_3$ ,  $^1J_{CF} = 32.14$  Hz), 32.38 (s,  $\beta$ -*NtBu*), 14.92 (d,  $PMe_3$ ,  $^1J_{PC} = 22.63$  Hz). The  $\alpha$ -*NtBu* and  $\alpha$ - $C(CF_3)_3$  resonances could not be observed.  $^{31}P\{^1H\}$  NMR ( $PhCF_3$  ( $C_6D_6$  insert), 242.9 MHz)  $\delta$  -1.43 (vbr s,  $\Delta\nu_{1/2} = 2236.40$  Hz).  $^{51}V\{^1H\}$  NMR ( $PhCF_3$  ( $C_6D_6$  insert), 157.7 MHz)  $\delta$  -810.15 (br s,  $\Delta\nu_{1/2} = 939.0$  Hz). IR ( $CaF_2$ , solution cell,  $PhCF_3$  subtracted,  $cm^{-1}$ ): Insufficient intensity above  $PhCF_3$  in nitrile absorption region.

**Preparation of  $VCl_2(PEt_3)_2(N^tBu)_2$  (4).** To a solution of  $VCl_2(N^tBu)(NTMS^tBu)$  (2.10 g, 6.2 mmol) in 50 mL of toluene was added triethylphosphine (2.1 equiv, 1.89 mL, 13.1 mmol) via syringe. After this addition, the reaction flask was fitted with a reflux condenser, and the reaction mixture was stirred for 16 h at reflux with a bath temperature of 125  $^\circ C$ . The reaction mixture was then cooled to room temperature and reduced to a residue in vacuo. The residue was extracted with HMDSO, and the combined extracts were filtered via cannula, and reduced in volume in vacuo until the product began to crystallize. After cooling the solution to  $-40^\circ C$  overnight and decantation, the product was recrystallized by the same method to afford analytically pure product in 83% yield (2.42 g) as large, light green blocks. Recrystallization from HMDSO at  $-40^\circ C$  afforded X-ray quality crystals.  $^1H$  NMR ( $C_6D_6$ , 600.1 MHz)  $\delta$  1.80 (unresolved m,  $P(CH_2CH_3)_3$ , 12H), 1.40 (s, *NtBu*), 1.10 (unresolved m,  $P(CH_2CH_3)_3$ , 18H).  $^{13}C\{^1H\}$  NMR ( $C_6D_6$ , 150.9 MHz)  $\delta$  68.43 (br s,  $\alpha$ -*NtBu*), 33.99 (s,  $\beta$ -*tBu*), 16.85 (br s,  $P(CH_2CH_3)_3$ ), 8.74 (br s,  $P(CH_2CH_3)_3$ ).  $^{31}P\{^1H\}$  NMR ( $C_6D_6$ , 242.9 MHz, 298 K)  $\delta$  26.79 (br s,  $\Delta\nu_{1/2} = 2051.66$  Hz).  $^{51}V\{^1H\}$  NMR ( $C_6D_6$ , 157.7 MHz)  $\delta$  -757.33 (br s,  $\Delta\nu_{1/2} = 11.78$  Hz). Anal. Calcd (%) for  $C_{40}H_{49}AlF_{36}N_3O_4P_2V$ : C, 32.91; H, 3.38; N, 2.88. Found: C, 32.67; H, 3.10; N, 2.84. IR (KBr,  $cm^{-1}$ ): 1413 (s), 1349 (s), 1228 (s), 1208 (s), 1033 (s), 761 (s), 750 (s), 715 (m), 685 (w), 586 (m), 468 (w). Mp = 66–68  $^\circ C$ .

**Preparation of  $[V(PEt_3)_2(N^tBu)_2][Al(PFTB)_4]$  (5).** Method A: To a slurry of  $Li[Al(PFTB)_4]$  (974 mg, 1 mmol) in 15 mL of DCE was added **4** (465 mg, 1 mmol) in 15 mL of DCE. The reaction mixture was stirred overnight at room temperature (rt), filtered through Celite, and reduced in volume until the product began to crystallize. After cooling the solution to  $-15^\circ C$  overnight, the title compound was afforded in 47% yield (650 mg) after decantation, as deep red blades.  $^1H$  NMR ( $PhCF_3$  ( $C_6D_6$  insert), 600.1 MHz)  $\delta$  1.46 (pseudo quintet (doublet of quartets),  $P(CH_2CH_3)_3$ , 12H), 1.25 (s, *NtBu*, 18H), 1.01 (pseudo quintet (doublet of triplets),  $P(CH_2CH_3)_3$ , 18H).  $^{13}C$  NMR ( $PhCF_3$  ( $C_6D_6$  insert), 150.9 MHz)  $\delta$  131.02 (q,  $C(CF_3)_3$ ,  $^1J_{CF} = 32.14$  Hz), 72.6\* ( $\alpha$ -*NtBu*), 32.73 (s,  $\beta$ -*tBu*), 16.19 (t,  $P(CH_2CH_3)_3$ ,  $^1J_{PC} = 7.39$  Hz), 16.04 (t,  $P(CH_2CH_3)_3$ ,  $^1J_{PC} = 8.63$  Hz), 7.84 (br s,  $P(CH_2CH_3)_3$ ). The  $\alpha$ - $C(CF_3)_3$  resonance.  $^{31}P\{^1H\}$  NMR ( $PhCF_3$  ( $C_6D_6$  insert), 242.9 MHz)  $\delta$  26.69 (vbr s,  $\Delta\nu_{1/2} = 2674.50$  Hz).  $^{51}V\{^1H\}$  NMR ( $PhCF_3$  ( $C_6D_6$  insert), 157.7 MHz)  $\delta$  -278.99 (br s,  $\Delta\nu_{1/2} = 80.78$  Hz). Anal. Calcd (%) for  $C_{36}H_{48}AlF_{36}N_2O_4P_2V$ : C, 30.96; H, 3.46; N, 2.01. Found: C, 30.75; H, 3.20; N, 2.06. IR (KBr,  $cm^{-1}$ ): 1417 (s), 1352 (m), 1300 (s), 1219 (s), 1168 (w), 1038 (w), 831 (w), 768 (w), 755 (w), 560 (w), 537 (w), 444 (w). Mp = 150  $^\circ C$  (dec.).

Method B: A scintillation vial was charged with  $Li[Al(PFTB)_4]$  (21 mg, 0.02 mmol) and  $\sim 300$   $\mu L$  of the appropriate solvent. To this slurry was added a solution of **4** (10 mg, 0.02 mmol) in  $\sim 150$   $\mu L$  of same solvent. On mixing, the solution shifted from green to deep red. The reaction mixture was agitated via pipet for 5 min and transferred via pipet to a J. Young NMR tube, in the case of a *protio*-solvent a sealed capillary filled with  $C_6D_6$  was included. The scintillation vials and pipettes were washed with a further  $\sim 150$   $\mu L$  of solvent and transferred to the J. Young NMR tube.



**Preparation of [V(PET)<sub>2</sub>(N<sup>t</sup>Bu)<sub>2</sub>(DMAP)][Al(PFTB)<sub>4</sub>] (6).** To a slurry of Li[Al(PFTB)<sub>4</sub>] (400 mg, 0.41 mmol) in 5 mL PhCF<sub>3</sub> was added sequentially 4-dimethylaminopyridine (1 equiv, 50 mg, 0.41 mmol) in 5 mL of PhCF<sub>3</sub> and **4** (1 equiv, 191 mg, 0.41 mmol) in 5 mL of PhCF<sub>3</sub> via cannula. After these additions, the reaction mixture was stirred for 1 h, during which time the solution became bright yellow. The reaction mixture was then filtered through Celite and reduced until the product began to crystallize. After cooling the solution to -15 °C overnight, the title compound was afforded in 50% yield (310 mg) after decantation, as yellow blocks. Recrystallization from PhCF<sub>3</sub> afforded X-ray quality crystals. <sup>1</sup>H NMR (PhCF<sub>3</sub> (C<sub>6</sub>D<sub>6</sub> insert), 600.1 MHz) δ 7.95 (d, ArH, 2H, J = 4.8 Hz), 6.39 (d, ArH, 2H, J = 6.0 Hz), 2.65 (s, Me, 6H), 1.28 (s with shoulder, N<sup>t</sup>Bu and P(CH<sub>2</sub>CH<sub>3</sub>)<sub>3</sub>, 30H), 0.91 (unresolved m, P(CH<sub>2</sub>CH<sub>3</sub>)<sub>3</sub>, 18H). <sup>13</sup>C NMR (PhCF<sub>3</sub> (C<sub>6</sub>D<sub>6</sub> insert), 150.9 MHz) δ 155.23 (s, Ar), 149.74 (s, Ar), 131.14 (q, C(CF<sub>3</sub>)<sub>3</sub>, <sup>1</sup>J<sub>CF</sub> = 32.29 Hz), 107.17 (s, Ar), 68.0\* (α-N<sup>t</sup>Bu), 38.22 (s, DMAP-Me), 33.97 (s, β-N<sup>t</sup>Bu), 16.74 (br s, P(CH<sub>2</sub>CH<sub>3</sub>)<sub>3</sub>), 8.09 (br s, P(CH<sub>2</sub>CH<sub>3</sub>)<sub>3</sub>). The α-C(CF<sub>3</sub>)<sub>3</sub> resonance could not be observed. <sup>31</sup>P{<sup>1</sup>H} NMR (PhCF<sub>3</sub> (C<sub>6</sub>D<sub>6</sub> insert), 242.9 MHz) δ 24.67 (vbr s, Δν<sub>1/2</sub> = 1800.53 Hz). <sup>51</sup>V{<sup>1</sup>H} NMR (PhCF<sub>3</sub> (C<sub>6</sub>D<sub>6</sub> insert), 157.7 MHz) δ -728.16 (br s, Δν<sub>1/2</sub> = 69.00 Hz). Anal. Calcd (%) for C<sub>43</sub>H<sub>58</sub>AlF<sub>36</sub>N<sub>4</sub>O<sub>4</sub>P<sub>2</sub>V: C, 34.01; H, 3.85; N, 3.65. Found: C, 33.94; H, 3.74; N, 3.72. IR (KBr, cm<sup>-1</sup>): 1622 (s), 1398 (s), 1353 (s), 1219 (s), 1169 (s), 1062 (m), 1037 (m), 1011 (m), 832 (m), 817 (m), 760 (m), 584 (w), 560 (w), 537 (m), 445 (m). Mp = 91 °C (dec.).

**Preparation of [V(PET)<sub>2</sub>(N<sup>t</sup>Bu)<sub>2</sub>(CNXyl)][Al(PFTB)<sub>4</sub>] (7).** To a solution of [V(PET)<sub>3</sub>(N<sup>t</sup>Bu)<sub>2</sub>][Al(PFTB)<sub>4</sub>] (184 mg, 0.13 mmol) in 5 mL of 1,2-dichloroethane was added 2,6-xylylisocyanide (1 equiv, 17 mg, 0.13 mmol) in 5 mL of DCE via cannula. After this addition, the reaction mixture was stirred for 12 h. The reaction mixture was then filtered via cannula and reduced until the product began to crystallize. After cooling the solution to -15 °C overnight, the title compound was afforded in 60% yield (120 mg) after decantation, as yellow-orange blades. <sup>1</sup>H NMR (PhCF<sub>3</sub> (C<sub>6</sub>D<sub>6</sub> insert), 600.1 MHz) δ 2.23 (s, Me, 6H), 1.68 (pseudo quintet (doublet of quartets), 12H, P(CH<sub>2</sub>CH<sub>3</sub>)<sub>3</sub>), 1.19 (s, N<sup>t</sup>Bu, 18H), 0.99 (pseudo quintet (doublet of triplets, P(CH<sub>2</sub>CH<sub>3</sub>)<sub>3</sub>, 18H). Aryl proton resonances could not be observed because of overlapping *protio*-solvent resonances. <sup>13</sup>C NMR (PhCF<sub>3</sub> (C<sub>6</sub>D<sub>6</sub> insert), 150.9 MHz) δ 159.67 (s, Ar), 134.30 (s, Ar), 130.38 (q, C(CF<sub>3</sub>)<sub>3</sub>, <sup>1</sup>J<sub>CF</sub> = 32.14 Hz), 118.81 (s, Ar), 96.57 (s, Ar), 70.5\* (α-N<sup>t</sup>Bu), 32.91 (unresolved q, β-N<sup>t</sup>Bu), 18.46 (dd, P(CH<sub>2</sub>CH<sub>3</sub>)<sub>3</sub>), <sup>1</sup>J<sub>PC</sub> = 11.92 Hz, <sup>3</sup>J<sub>PC</sub> = 9.20 Hz), 17.24 (s, Ar-ortho-Me), 7.57 (s, P(CH<sub>2</sub>CH<sub>3</sub>)<sub>3</sub>). The α-C(CF<sub>3</sub>)<sub>3</sub> resonance could not be observed. <sup>31</sup>P{<sup>1</sup>H} NMR (PhCF<sub>3</sub> (C<sub>6</sub>D<sub>6</sub> insert), 242.9 MHz) δ 32.26 (vbr s, Δν<sub>1/2</sub> = 1803.50 Hz). <sup>51</sup>V{<sup>1</sup>H} NMR (PhCF<sub>3</sub> (C<sub>6</sub>D<sub>6</sub> insert), 157.7 MHz) δ -903.43 (br s, Δν<sub>1/2</sub> = 109.39 Hz). Anal. Calcd (%) for C<sub>45</sub>H<sub>57</sub>AlF<sub>36</sub>N<sub>3</sub>O<sub>4</sub>P<sub>2</sub>V: C, 35.38; H, 3.76; N, 2.75. Found: C, 35.27; H, 3.61; N, 2.70. IR (KBr, cm<sup>-1</sup>): 2156 (m), 1353 (s), 1277 (s), 1220 (s), 1163 (m), 1034 (w), 832 (w), 770 (w), 754 (w), 560 (w), 537 (w), 445 (m). Mp = 110 °C (dec.).

**Observation of [V(PET)<sub>2</sub>(N<sup>t</sup>Bu)<sub>2</sub>(CO)][Al(PFTB)<sub>4</sub>] (8).** A scintillation vial was charged with Li[Al(PFTB)<sub>4</sub>] (21 mg, 0.02 mmol) and ~300 μL of PhCF<sub>3</sub>. To this slurry was added a solution of **3** (10 mg, 0.02 mmol) in ~150 μL in PhCF<sub>3</sub>. On mixing, the solution color shifted from green to deep red. The reaction mixture was agitated via pipet for 5 min and transferred via pipet to a J. Young NMR tube charged with a sealed capillary filled with C<sub>6</sub>D<sub>6</sub>. The scintillation vials and pipettes were washed with a further ~150 μL of solvent and then the combined solution was transferred to the J. Young NMR tube. This NMR tube was removed from the box, attached to a line, and degassed by 3 freeze-pump-thaw cycles. Carbon monoxide (1 atm, excess) was added to the thawed solution via the vacuum manifold. <sup>1</sup>H NMR (PhCF<sub>3</sub> (C<sub>6</sub>D<sub>6</sub> insert), 600.1 MHz) δ 1.52 (unresolved m, 12H, P(CH<sub>2</sub>CH<sub>3</sub>)<sub>3</sub>), 1.24 (s, N<sup>t</sup>Bu, 18H), 1.01 (unresolved m, P(CH<sub>2</sub>CH<sub>3</sub>)<sub>3</sub>, 18H). <sup>13</sup>C NMR (PhCF<sub>3</sub> (C<sub>6</sub>D<sub>6</sub> insert), 150.9 MHz) δ 131.18 (q, C(CF<sub>3</sub>)<sub>3</sub>, <sup>1</sup>J<sub>CF</sub> = 32.29 Hz), 32.07 (s, β-N<sup>t</sup>Bu), 16.51 (unresolved m, P(CH<sub>2</sub>CH<sub>3</sub>)<sub>3</sub>), 7.89 (s, P(CH<sub>2</sub>CH<sub>3</sub>)<sub>3</sub>). The α-C(CF<sub>3</sub>)<sub>3</sub> resonance could not be observed. <sup>31</sup>P{<sup>1</sup>H} NMR (PhCF<sub>3</sub> (C<sub>6</sub>D<sub>6</sub> insert), 242.9 MHz) δ 25.39 (vbr s, Δν<sub>1/2</sub> = 2533.94 Hz). <sup>51</sup>V{<sup>1</sup>H}

NMR (PhCF<sub>3</sub> (C<sub>6</sub>D<sub>6</sub> insert), 157.7 MHz) δ -843.71 (pseudo d, <sup>1</sup>J<sub>VP</sub> = 225.13 Hz, Δν<sub>1/2</sub> = 233.93 Hz). IR (CaF<sub>2</sub>, solution cell, PhCF<sub>3</sub> subtracted, cm<sup>-1</sup>): 2015 (s). (**8**-<sup>13</sup>C) was prepared similarly. <sup>13</sup>C NMR (PhCF<sub>3</sub> (C<sub>6</sub>D<sub>6</sub> insert), 150.9 MHz) δ 228.36 (br s, <sup>13</sup>CO). <sup>51</sup>V{<sup>1</sup>H} NMR (PhCF<sub>3</sub> (C<sub>6</sub>D<sub>6</sub> insert), 157.7 MHz) δ -845.06 (br s, Δν<sub>1/2</sub> = 531.05 Hz). IR (CaF<sub>2</sub>, solution cell, PhCF<sub>3</sub> subtracted, cm<sup>-1</sup>): 1970 (s).

**General Remarks on the Determination of Molecular Structure by XRD.** XRD data were collected using either Bruker AXS three-circle or Bruker AXS Microstar kappa-geometry diffractometers with either graphite-monochromated Mo-Kα radiation (λ = 0.71073 Å) or HELIOS-monochromated Cu-Kα radiation (λ = 1.54178 Å). A single crystal of appropriate size was coated in Paratone-N oil and mounted on a Cryo loop. The loop was transferred to a diffractometer equipped with a CCD area detector,<sup>100</sup> centered in the beam, and cooled by an Oxford Cryostream 700 LT device. Preliminary orientation matrices and cell constants were determined by collection of three sets of 40, 5 s frames or three sets of 30, 10 s frames, followed by spot integration and least-squares refinement. COSMO was used to determine an appropriate data collection strategy, and the raw data were integrated using SAINT.<sup>101</sup> Cell dimensions reported were calculated from all reflections with I > 10 σ. The data were corrected for Lorentz and polarization effects; no correction for crystal decay was applied. Data were analyzed for agreement and possible absorption using XPREP.<sup>102</sup> An absorption correction based on comparison of redundant and equivalent reflections was applied using SADABS.<sup>103</sup> Structures were solved by direct methods with the aid of successive difference Fourier maps and were refined on F<sup>2</sup> using the SHELXTL 5.0 software package. All non-hydrogen atoms were refined anisotropically; all hydrogen atoms were included into the model at their calculated positions and refined using a riding model. Additional details for compounds **2**, **4**, and **6** are contained within the cif files. For all structures, R<sub>1</sub> = Σ(|F<sub>o</sub>l - |F<sub>c</sub>l|) / Σ(|F<sub>o</sub>l|); wR<sub>2</sub> = [Σ{w(F<sub>o</sub><sup>2</sup> - F<sub>c</sub><sup>2</sup>)<sup>2</sup>} / Σ{w(F<sub>o</sub><sup>2</sup>)<sup>2</sup>}]<sup>1/2</sup>.

**Computational Methods.** DFT calculations were performed using the Gaussian09 software package.<sup>104</sup> Geometries were fully optimized and converged to at least the default geometric convergence criteria. The use of symmetry was explicitly turned off for all computations. Frequencies were calculated analytically at 298.15 K and 1 atm in the gas phase, and structures were considered true minima if they did not exhibit imaginary modes. The hybrid functional used was B3LYP.<sup>105–107</sup> A LANL2DZ small core ECP and its appropriate valence basis set was used for V.<sup>108–111</sup> The remaining atoms were treated with Pople's 6-31G(d,p) double-ζ split-valence basis using the 5 spherical d orbital functions instead of the default.<sup>112</sup> Optimized structures were subjected to vibrational frequency analysis and visualized using the Gaussian09 software package. Orbital contributions were determined with pop = orbitals. Atom Cartesian coordinates are listed in Supporting Information, Table S1.

## ■ ASSOCIATED CONTENT

### 📄 Supporting Information

Crystallographic and DFT details, and CIF files. This material is available free of charge via the Internet at <http://pubs.acs.org>.

## ■ AUTHOR INFORMATION

### Corresponding Author

\*E-mail: [arnold@berkeley.edu](mailto:arnold@berkeley.edu) (J.A.), [rbergman@berkeley.edu](mailto:rbergman@berkeley.edu) (R.G.B.), and [fdtoste@berkeley.edu](mailto:fdtoste@berkeley.edu) (F.D.T.).

### Notes

The authors declare no competing financial interest.

## ■ ACKNOWLEDGMENTS

H.S.LaP. acknowledges the support of the NSF for a predoctoral fellowship and the UCB Department of Chemistry for the Dauben Fellowship. We would like to thank Drs. Jamin Krinsky, Xinzhen Yang, Christopher Canlas, and Antonio G.

DiPasquale for their experimental assistance, and Prof. Richard A. Andersen, Dr. Gregory Nocton, Dr. Neil C. Tomson, and Thomas L. Gianetti for helpful discussions. This work was supported by the AFOSR (11RSA093). Molecular modeling was performed at the UC Berkeley Molecular Graphics and Computation Facility, directed by Dr. K. Durkin and operated with equipment funds from NSF Grant CHE-0233882 and donations from Dell.

## REFERENCES

- (1) Chirik, P. J.; Knobloch, D. J.; Lobkovsky, E. *J. Am. Chem. Soc.* **2010**, *132*, 10553.
- (2) Cloke, F. G. N.; Frey, A. S.; Hitchcock, P. B.; Day, I. J.; Green, J. C.; Aitken, G. *J. Am. Chem. Soc.* **2008**, *130*, 13816.
- (3) Cloke, F. G. N.; Summerscales, O. T.; Hitchcock, P. B.; Green, J. C.; Hazari, N. *J. Am. Chem. Soc.* **2006**, *128*, 9602.
- (4) Summerscales, O. T.; Cloke, F. G. N.; Hitchcock, P. B.; Green, J. C.; Hazari, N. *Science* **2006**, *311*, 829.
- (5) Frey, A. S. P.; Cloke, F. G. N.; Coles, M. P.; Maron, L.; Davin, T. *Angew. Chem., Int. Ed.* **2011**, *50*, 6881.
- (6) Martínez-Salvador, S.; Forniés, J.; Martín, A.; Menjón, B. *Chem.—Eur. J.* **2011**, *17*, 8085.
- (7) Maron, L.; Perrin, L.; Eisenstein, O.; Andersen, R. A. *J. Am. Chem. Soc.* **2002**, *124*, 5614.
- (8) Werkema, E. L.; Maron, L.; Eisenstein, O.; Andersen, R. A. *J. Am. Chem. Soc.* **2007**, *129*, 6662.
- (9) Eisenstein, O.; Maron, L.; Andersen, R. A. *Organometallics* **2009**, *28*, 3629.
- (10) Williams, V. A.; Manke, D. R.; Cundari, T. R.; Wolczanski, P. T. *Inorg. Chim. Acta* **2011**, *369*, 203.
- (11) Labinger, J. A.; West, N. M.; Miller, A. J. M.; Bercaw, J. E. *Coord. Chem. Rev.* **2011**, *255*, 881.
- (12) Labinger, J. A.; Miller, A. J. M.; Bercaw, J. E. *J. Am. Chem. Soc.* **2010**, *132*, 3301.
- (13) Labinger, J. A.; Miller, A. J. M.; Bercaw, J. E. *Organometallics* **2010**, *29*, 4499.
- (14) Labinger, J. A.; Miller, A. J. M.; Bercaw, J. E. *J. Am. Chem. Soc.* **2008**, *130*, 11874.
- (15) Chirik, P. J.; Knobloch, D. J.; Lobkovsky, E. *Nat. Chem.* **2010**, *2*, 30.
- (16) Knobloch, D. J., Ph.D. Thesis, Cornell University, Ithaca, NY, 2011.
- (17) Tomson, N. C.; Arnold, J.; Bergman, R. G. *Organometallics* **2010**, *29*, 5010.
- (18) Gianetti, T. L.; Tomson, N. C.; Arnold, J.; Bergman, R. G. *J. Am. Chem. Soc.* **2011**, *133* (38), 14904–14907.
- (19) Demerseman, B.; Pankowski, M.; Bouquet, G.; Bigorgne, M. J. *Organomet. Chem.* **1976**, *117*, C10.
- (20) Calderazzo, F.; Pampaloni, G.; Tripepi, G. *Organometallics* **1997**, *16*, 4943.
- (21) Manriquez, J. M.; Mcalister, D. R.; Sanner, R. D.; Bercaw, J. E. *J. Am. Chem. Soc.* **1978**, *100*, 2716.
- (22) Manriquez, J. M.; Mcalister, D. R.; Sanner, R. D.; Bercaw, J. E. *J. Am. Chem. Soc.* **1976**, *98*, 6733.
- (23) Roddick, D. M.; Fryzuk, M. D.; Seidler, P. F.; Hillhouse, G. L.; Bercaw, J. E. *Organometallics* **1985**, *4*, 97.
- (24) Procopio, L. J.; Carroll, P. J.; Berry, D. H. *Polyhedron* **1995**, *14*, 45.
- (25) Howard, W. A.; Parkin, G.; Rheingold, A. L. *Polyhedron* **1995**, *14*, 25.
- (26) Howard, W. A.; Trnka, T. M.; Parkin, G. *Organometallics* **1995**, *14*, 4037.
- (27) Brackemeyer, T.; Erker, G.; Frohlich, R. *Organometallics* **1997**, *16*, 531.
- (28) Antonelli, D. M.; Tjaden, E. B.; Stryker, J. M. *Organometallics* **1994**, *13*, 763.
- (29) Guram, A. S.; Swenson, D. C.; Jordan, R. F. *J. Am. Chem. Soc.* **1992**, *114*, 8991.
- (30) Guo, Z. Y.; Swenson, D. C.; Guram, A. S.; Jordan, R. F. *Organometallics* **1994**, *13*, 766.
- (31) Reynoud, J. F.; Leboeuf, J. F.; Leblanc, J. C.; Moise, C. *Organometallics* **1986**, *5*, 1863.
- (32) Burckhardt, U.; Tilley, T. D. *J. Am. Chem. Soc.* **1999**, *121*, 6328. Tilley has proposed  $\pi$  back-bonding from the filled  $\pi$  symmetry metal-Cp orbitals to CO, but argues convincingly in favor of Ta-Si  $\sigma$  to  $\pi^*$  interaction in the complex presented in this communication.
- (33) Brennan, J. G.; Andersen, R. A.; Robbins, J. L. *J. Am. Chem. Soc.* **1986**, *108*, 335.
- (34) Parry, J.; Carmona, E.; Coles, S.; Hursthouse, M. *J. Am. Chem. Soc.* **1995**, *117*, 2649.
- (35) Conejo, M. D.; Parry, J. S.; Carmona, E.; Schultz, M.; Brennan, J. G.; Beshouri, S. M.; Andersen, R. A.; Rogers, R. D.; Coles, S.; Hursthouse, M. *Chem.—Eur. J.* **1999**, *5*, 3000.
- (36) Foster, S. C.; Mckellar, A. R. W.; Sears, T. J. *J. Chem. Phys.* **1984**, *81*, 578.
- (37) Davies, P. B.; Hamilton, P. A.; Rothwell, W. J. *J. Chem. Phys.* **1984**, *81*, 1598.
- (38) Strandberg, M. W. P.; Pearsall, C. S.; Weiss, M. T. *J. Chem. Phys.* **1949**, *17*, 429.
- (39) Sanchez, R.; Arrington, C.; Arrington, C. A. *J. Am. Chem. Soc.* **1989**, *111*, 9110.
- (40) Selg, P.; Brintzinger, H. H.; Andersen, R. A.; Horvath, I. T. *Angew. Chem., Int. Ed. Engl.* **1995**, *34*, 791.
- (41) Selg, P.; Brintzinger, H. H.; Schultz, M.; Andersen, R. A. *Organometallics* **2002**, *21*, 3100.
- (42) Bodenbinder, M.; BalzerJollenbeck, G.; Willner, H.; Batchelor, R. J.; Einstein, F. W. B.; Wang, C.; Aubke, F. *Inorg. Chem.* **1996**, *35*, 82.
- (43) Willner, H.; Bodenbinder, M.; Brochler, R.; Hwang, G.; Rettig, S. J.; Trotter, J.; von Ahsen, B.; Westphal, U.; Jonas, V.; Thiel, W.; Aubke, F. *J. Am. Chem. Soc.* **2001**, *123*, 588.
- (44) Willner, H.; Aubke, F. *Inorg. Chem.* **1990**, *29*, 2195.
- (45) Hurlburt, P. K.; Rack, J. J.; Luck, J. S.; Dec, S. F.; Webb, J. D.; Anderson, O. P.; Strauss, S. H. *J. Am. Chem. Soc.* **1994**, *116*, 10003.
- (46) Hurlburt, P. K.; Rack, J. J.; Dec, S. F.; Anderson, O. P.; Strauss, S. H. *Inorg. Chem.* **1993**, *32*, 373.
- (47) Hurlburt, P. K.; Anderson, O. P.; Strauss, S. H. *J. Am. Chem. Soc.* **1991**, *113*, 6277.
- (48) Hakansson, M.; Jagner, S. *Inorg. Chem.* **1990**, *29*, 5241.
- (49) Dewar, J. S. *Bull. Chem. Soc. Fr.* **1951**, *18*, C71.
- (50) Chatt, J.; Duncanson, L. A. *J. Chem. Soc.* **1953**, 2939.
- (51) La Pierre, H. S.; Arnold, J.; Toste, F. D. *Angew. Chem., Int. Ed.* **2011**, *50*, 3900.
- (52) Nugent, W. A.; Mayer, J. M. *Metal-Ligand Multiple Bonds*; Wiley: New York, 1988.
- (53) Cockcroft, J. K.; Gibson, V. C.; Howard, J. A. K.; Poole, A. D.; Siemeling, U.; Wilson, C. *J. Chem. Soc., Chem. Commun.* **1992**, 1668.
- (54) Poole, A. D.; Gibson, V. C.; Clegg, W. *J. Chem. Soc., Chem. Commun.* **1992**, 237.
- (55) Glueck, D. S.; Green, J. C.; Michelman, R. I.; Wright, I. N. *Organometallics* **1992**, *11*, 4221.
- (56) Williams, D. S.; Schofield, M. H.; Anhaus, J. T.; Schrock, R. R. *J. Am. Chem. Soc.* **1990**, *112*, 6728.
- (57) Williams, D. S.; Schofield, M. H.; Schrock, R. R. *Organometallics* **1993**, *12*, 4560.
- (58) Albright, T. A.; Burdett, J. K.; Whangbo, M. H. *Orbital Interactions in Chemistry*; John Wiley & Sons: New York, 1985.
- (59) Lauher, J. W.; Hoffmann, R. *J. Am. Chem. Soc.* **1976**, *98*, 1729.
- (60) Brintzinger, H. H.; Lohr, L. L.; Wong, K. L. T. *J. Am. Chem. Soc.* **1975**, *97*, 5146.
- (61) Chirik, P. J. *Organometallics* **2010**, *29*, 1500.
- (62) Togni, A.; Halterman, R. L., Eds.; *Metalloenes: Synthesis, Reactivity, Application*; Wiley-VCH: New York, 1998.
- (63) Kealy, T. J.; Pauson, P. L. *Nature* **1951**, *168*, 1039.
- (64) Wilkinson, G.; Rosenblum, M.; Whiting, M. C.; Woodward, R. B. *J. Am. Chem. Soc.* **1952**, *74*, 2125.
- (65) Wigley, D. E. *Prog. Inorg. Chem.* **1994**, 239.

- (66) Dyer, P. W.; Gibson, V. C.; Howard, J. A. K.; Whittle, B.; Wilson, C. J. *Chem. Soc., Chem. Commun.* **1992**, 1666.
- (67) Khalimon, A. Y.; Simionescu, R.; Kuzmina, L. G.; Howard, J. A. K.; Nikonov, G. I. *Angew. Chem., Int. Ed.* **2008**, *47*, 7701.
- (68) Nikonov, G. I.; Khalimon, A. Y.; Simionescu, R. *J. Am. Chem. Soc.* **2011**, *133*, 7033.
- (69) Mountford, P.; Ignatov, S. K.; Khalimon, A. Y.; Rees, N. H.; Razuvaev, A. G.; Nikonov, G. I. *Inorg. Chem.* **2009**, *48*, 9605.
- (70) Green, J. C.; Khalimon, A. Y.; Holland, J. P.; Kowalczyk, R. M.; McInnes, E. J. L.; Mountford, P.; Nikonov, G. I. *Inorg. Chem.* **2008**, *47*, 999.
- (71) Ignatov, S. K.; Rees, N. H.; Dubberley, S. R.; Razuvaev, A. G.; Mountford, P.; Nikonov, G. I. *Chem. Commun.* **2004**, 952.
- (72) DeWith, J.; Horton, A. D. *Angew. Chem., Int. Ed. Engl.* **1993**, *32*, 903.
- (73) Schaller, C. P.; Wolczanski, P. T. *Inorg. Chem.* **1993**, *32*, 131.
- (74) Nolin, K. A.; Ahn, R. W.; Kobayashi, Y.; Kennedy-Smith, J. J.; Toste, F. D. *Chem.—Eur. J.* **2010**, *16*, 9555.
- (75) Nolin, K. A.; Krumper, J. R.; Pluth, M. D.; Bergman, R. G.; Toste, F. D. *J. Am. Chem. Soc.* **2007**, *129*, 14684.
- (76) Nolin, K. A.; Ahn, R. W.; Toste, F. D. *J. Am. Chem. Soc.* **2005**, *127*, 12462.
- (77) Kennedy-Smith, J. J.; Nolin, K. A.; Gunterman, H. P.; Toste, F. D. *J. Am. Chem. Soc.* **2003**, *125*, 4056.
- (78) Hoyt, H. M.; Michael, F. E.; Bergman, R. G. *J. Am. Chem. Soc.* **2004**, *126*, 1018.
- (79) Tomson, N. C.; Arnold, J.; Bergman, R. G. *Organometallics* **2010**, *29*, 2926.
- (80) Walsh, P. J.; Hollander, F. J.; Bergman, R. G. *J. Am. Chem. Soc.* **1988**, *110*, 8729.
- (81) Addison, A. W.; Rao, T. N.; Reedijk, J.; Vanrijn, J.; Verschoor, G. C. *J. Chem. Soc., Dalton Trans.* **1984**, 1349.
- (82) Chao, Y. W.; Wexler, P. A.; Wigley, D. E. *Inorg. Chem.* **1990**, *29*, 4592.
- (83) DeWith, J.; Horton, A. D.; Orpen, A. G. *Organometallics* **1990**, *9*, 2207.
- (84) DeWith, J.; Horton, A. D.; Orpen, A. G. *Organometallics* **1993**, *12*, 1493.
- (85) Krossing, I. *Chem.—Eur. J.* **2001**, *7*, 490.
- (86) Helm, L.; Bodizs, G.; Raabe, I.; Scopelliti, R.; Krossing, I. *Dalton Trans.* **2009**, 5137, and references therein.
- (87) Preuss, F.; Towae, W. Z. *Natforsch. B: Anorg. Allg. Chem.* **1981**, *36*, 1130.
- (88) Massa, W.; Wocadlo, S.; Lotz, S.; Dehnicke, K. Z. *Anorg. Allg. Chem.* **1990**, 589, 79.
- (89) Kilgore, U. J.; Karty, J. A.; Pink, M.; Gao, X.; Mindiola, D. J. *Angew. Chem., Int. Ed.* **2009**, *48*, 2394.
- (90) Mathieson, T.; Schier, A.; Schmidbaur, H. *J. Chem. Soc., Dalton Trans.* **2001**, 1196.
- (91) Crabtree, R. H. *The Organometallic Chemistry of the Transition Metals*, 4th ed.; John Wiley & Sons, Inc.: Hoboken, NJ, 2005.
- (92) Carofiglio, T.; Floriani, C.; Chiesivilla, A.; Guastini, C. *Inorg. Chem.* **1989**, *28*, 4417.
- (93) Ellis, J. E.; Allen, J. M. *J. Organomet. Chem.* **2008**, *693*, 1536.
- (94) Ahlers, W.; Erker, G.; Frohlich, R. *J. Organomet. Chem.* **1998**, *571*, 83.
- (95) Tolman, C. A. *Chem. Rev.* **1977**, *77*, 313.
- (96) Schafer, D. F.; Wolczanski, P. T. *J. Am. Chem. Soc.* **1998**, *120*, 4881.
- (97) Toomey, H. E.; Pun, D.; Veiros, L. F.; Chirik, P. J. *Organometallics* **2008**, *27*, 872.
- (98) Andersen, R. A. *Personal Communication*. H<sub>2</sub> addition to Cp<sup>\*</sup>2Ti(NPh).
- (99) Cundari, T. R. *J. Am. Chem. Soc.* **1994**, *116*, 340.
- (100) SMART: Area-Detector Software package; Bruker Analytical X-ray Systems, Inc: Madison, WI, 2001–2003.
- (101) SAINT: SAX Area-Detector Integration Program, V6.40; Bruker Analytical X-ray Systems, Inc: Madison, WI, 2003.
- (102) XPREP; Bruker Analytical X-ray Systems, Inc: Madison, WI, 2003.
- (103) SADABS: Bruker-Nonius Area Detector Scaling and Absorption, V2.05; Bruker Analytical X-ray Systems, Inc: Madison, WI, 2003.
- (104) Frisch, M. J. et al. *Gaussian 09*, Revision A.1; Gaussian, Inc.: Wallingford, CT, 2009; see Supporting Information for full reference.
- (105) Becke, A. D. *Phys. Rev. A* **1988**, *38*, 3098.
- (106) Lee, C. T.; Yang, W. T.; Parr, R. G. *Phys. Rev. B* **1988**, *37*, 785.
- (107) Stephens, P. J.; Devlin, F. J.; Chabalowski, C. F.; Frisch, M. J. *J. Phys. Chem.* **1994**, *98*, 11623.
- (108) Dunning Jr., T. H.; Hay, P. J. In *Modern Theoretical Chemistry*; Schaefer, H. F., III, Ed.; Plenum: New York, 1976; Vol. 3, pp 1–28.
- (109) Hay, P. J.; Wadt, W. R. *J. Chem. Phys.* **1985**, *82*, 270.
- (110) Wadt, W. R.; Hay, P. J. *J. Chem. Phys.* **1985**, *82*, 284.
- (111) Hay, P. J.; Wadt, W. R. *J. Chem. Phys.* **1985**, *82*, 299.
- (112) Hariharan, P. C.; Pople, J. A. *Theor. Chim. Acta* **1973**, *28*, 213.